ACCURACY OF OPEN MRI FOR GUIDING INJECTION OF THE EQUINE DEEP DIGITAL FLEXOR TENDON WITHIN THE HOOF.

By

Lauren M. Groom

Thesis submitted to the faculty of the Virginia Polytechnic Institute and State University in partial fulfillment of the requirements for the degree of

Master of Science

In

Biomedical and Veterinary Sciences

Jennifer G. Barrett

Nathaniel A. White II

M. Norris Adams

April 13th 2017

Leesburg, Virginia

Keywords: deep digital flexor tendon, injection, MRI, stem cells

ACCURACY OF OPEN MRI FOR GUIDING INJECTION OF THE EQUINE DEEP DIGITAL FLEXOR TENDON WITHIN THE HOOF.

Lauren M. Groom

ABSTRACT

Lesions of the distal deep digital flexor tendon (DDFT) are frequently diagnosed using magnetic resonance imaging (MRI) in horses with foot pain. The prognosis for horses with DDFT lesions to return to previous levels of performance is poor. Treatment options are limited; consisting of conservative therapy, desmotomy of the accessory ligament of the deep digital flexor tendon, injection of the digital sheath or navicular bursa, navicular bursoscopy or intralesional injection. Intralesional injection of biologic therapeutics shows promise in tendon healing, with increased number of experimental and clinical studies finding positive results. However, accurate injection of DDFT lesions within the hoof is difficult and requires general anesthesia. The Hallmarq open, low-field MRI unit was used to develop an MRI-guided technique to inject structures within the hoof. This procedure has been previously reported for injecting the collateral ligaments of the distal interphalangeal joint. Four clinical cases of deep digital flexor tendinopathy have been treated with MRI-guided injections using a similar technique.

The aim of this study was to evaluate accuracy of a technique for injection of the deep digital flexor tendon within the hoof using MRI-guidance, which could be performed in standing patients. We hypothesized that injection of the DDFT within the hoof could be accurately guided using open low-field MRI to target either the lateral or medial lobe at a specific location. Ten cadaver limbs were positioned in an open, low-field MRI unit to mimic a standing horse. Each DDFT lobe was assigned to have a proximal (adjacent to the proximal aspect of the navicular bursa) or distal (adjacent to the navicular bone) injection. A titanium needle was inserted into each tendon lobe, guided by T1-weighted transverse images acquired simultaneously during injection. Oil-based colored dye was injected as a marker. Post-injection MRI and gross sections were assessed by three blinded investigators experienced in equine MRI. The success of injection as evaluated on gross section was 85% (70% proximal, 100% distal). The success of injection as evaluated by MRI was 65% (60% proximal, 70% distal). There was no significant difference between the success of injecting the medial *versus* lateral lobe. The major limitation of this study was the use of cadaver limbs with normal tendons. The authors concluded that injection of the

DDFT within the hoof is possible using MRI guidance. Future work should be focused on using the techniqe in live horses with tendon lesions, and more clinical studies are needed to determine the most efficacious biologic therapeutic for tendon healing.

ACCURACY OF OPEN MRI FOR GUIDING INJECTION OF THE EQUINE DEEP DIGITAL FLEXOR TENDON WITHIN THE HOOF.

Lauren M. Groom

GENERAL AUDIENCE ABSTRACT

The deep digital flexor tendon is a commonly injured soft tissue structure in horses. This tendon inserts on the distal phalanx, within the hoof capsule. At this level, lesions of this tendon are commonly diagnosed with magnetic responance imaging (MRI). Treatment options are limited and consist of stall rest, supportive shoeing and a rehabilitation program. The prognosis for horses to return to previous levels of work is poor. For specific lesions of the tendon, surgery can be performed to explore the navicular bursa which allows access to the dorsal surface of the tendon. Other treatment options include injection of corticosteroids in the digital tendon sheath or navicular bursa or intralesional injection of various biological therapeutics such as stem cells. In recent years, there has been increasing use of biological therapeutics for tendon injury. Research in experimental and clinical studies in horses has shown promise in using stem cells to improve the healing of tendon injuries. However, as the deep digital flexor tendon is not visible using ultrasonography at its most distal aspect within the hoof capsule, alternative techniques are needed to guide placement of a needle. Currently, these other techniques are difficult and require general anesthesia. The Hallmarq open, low-field MRI unit allows for MRI examinations to be performed in the standing horse, which decreases cost, staff involved and risks. We have developed a technique which utilizes open, low-field MRI to guide injection of the deep digital flexor tendon within the hoof capsule, that can be performed in standing horses. This study describes the technique in cadaver limbs and assesses the accuracy of targeting a specific portion of the tendon with the injection. Utilizing low-field MRI a technique was developed to guide injection of the deep digital flexor tendon within the hoof capsule, performed in standing horses. The results suggest that the technique is accurate when used in standing horses to inject the deep digital flexor tendon within the hoof.

Acknowledgements

I would first like to acknowledge the Virginia-Maryland College of Veterinary Medicine's Veterinary Memorial Fund for funding this project. I would like to thank Elaine Meilahn (EM) for her assistance in image analysis, and her overall dedication to teaching and research at Marion duPont Scott Equine Medical Center. I would like to sincerely thank my committee members for their continued involvement and assistance with this project. Dr. Norris Adams provided valuable advice when designing the study protocol and has since remained a voice of clinical reason. Dr. Nathaniel White was of great assistance in learning about MRI protocols, and has provided insight into the clinical application of MRI-guided injection techniques. Dr. Jennifer Barrett has guided me through the research process, from grant writing, to statistical analysis, manuscript preparation and the presentation of my results at conferences. Without her mentorship this Masters project would not have been possible. Lastly I would like to thank my husband, Michael, for his ongoing support of my professional career and aspirations, and his constant encouragment to work hard and be thankful for what we have.

Attributions

Several colleagues aided in the research and writing of this thesis. A brief description of their background and their contributions are included here.

Jennifer G. Barrett – MS, PhD, DVM, Diplomate ACVS, Diplomate ACVSMR (Marion duPont Scott Equine Medical Center, Virginia-Maryland College of Veterinary Medicine) is the primary advisor and committee chairperson. Dr. Barrett's primary research interest is regenerative medicine and tissue engineering. Dr. Barrett has earned a PhD in molecular biology and has extensive experience in stem cell research. She played a vital role in the overall project design, data analysis and interpretation and review of the thesis.

Nathaniel A. White II – DVM, MS, Diplomate ACVS (Marion duPont Scott Equine Medical Center, Virginia-Maryland College of Veterinary Medicine) is a committee member. Dr. White has extensive experience in the diagnosis and treatment of equine tendon and ligament injury, especially in diagnosing injury with low field MRI. He contributed significantly to data analysis and review of the thesis.

M. Norris Adams- DVM, Diplomate ACVS, Diplomate ACVSMR (Marion duPont Scott Equine Medical Center, Virginia-Maryland College of Veterinary Medicine) is a committee member. Dr. Adams has extensive clinical experience in the treatment of equine tendon and ligament injury. He contributed significantly to design of the specimen construct, data analysis and review of the thesis.

Table of contents

Front Matter

Acknowledgements……v

Attributions……vi

Table Of Contents……vii

List of Figures ……ix

List of Abbreviations……x

Overview of Thesis……1

Chapter 1……3

Literature Review……3

Tendon composition, structure & biomechanical properties ……3

Composition……3

Structure……4

Biomechanics……6

Changes with age and exercise ……8

Tendon injury and repair……9

Tendinopathy……10

Equine deep digital flexor tendinopathy……11

Deep digital flexor tendon anatomy and function……11

Pathophysiology……13

Incidence……15

Diagnosis of deep digital flexor tendinopathy……18

Clinical examination……18

Diagnostic imaging……18

Advanced imaging……20

Interventional imaging……25

Treatment & prognosis……28

Regenerative therapeutics……32

Stem cells…… 33

Introduction……33

Bone marrow-derived MSCs.....35
Adipose-derived MSCs.....37
Fetal-like and embryonic-like stem cells 39
MSC concentrates 40
PRP.....41
Conclusions.....44
Chapter 2.....45
Manuscript: Accuracy of Open MRI for Guiding Injection of the Equine Deep Digital Flexor Tendon within the Hoof......45
Abstract.....45
Introduction.....46
Materials and methods.....48
Results.....53
Discussion.....55
Conclusions.....61
References.....63

List Of Figures

Chapter 1

Figure 1: Tendon structure.....5
Figure 2. The stress-strain curve.....6
Figure 3: The hysteresis loop: loading and unloading curves are not overlapping due to energy loss during unloading. This energy equals the area between the two curves. With repeated loading, the curve moves to the right as the tendon becomes more elastic.....7

Chapter 2

Figure 1- A clinical case of deep digital flexor tendinopathy being injected with bone marrow-derived MSCs using open, low-field MRI guidance.....48
Figure 2- Cadaver specimen prepared and positioned to mimic the configuration of a standing, sedated horse.....50
Figure 3A- Transverse T1-weighted MRI slice showing the signal void due to needle artifact (arrow) approaching lateral lobe of DDFT.....51
Figure 3B- Sagittal T1-weighted MRI slice showing needle artifact (arrow) in DDFT at the proximal location.....51
Figure 4A- Gross specimen in transverse section demonstrating a successful distal injection. Blue dye is indicated by the arrow. Note the blue dye staining in the navicular bursa (star).....55
Figure 4B- Gross specimen in transverse section demonstrating a successful proximal injection. Orange dye is indicated by the long arrow. Note the blue dye staining in the digital sheath (star) and needle tract (short arrow) in the other tendon lobe.....55
Figure 5A- Transverse, T1-weighted MRI image of a successful distal injection. Hyperintense oil is indicated by the arrow.....55
Figure 5B- Transverse, T1-weighted MRI image of a successful proximal injection. Hyperintense oil is indicated by the arrow.....55
Graph 1- Procedure time for each injection in chronological order. Time was recorded from moment needle penetrated skin to the moment the needle was removed.....53
Graph 2- Location of synovial structure involvement in each sample.....54

List of Abbreviations

DDFT	Deep digital flexor tendon
SDFT	Superficial digital flexor tendon
CDET	Common digital extensor tendon
DSIL	Distal sesamoidean impar ligament
CSL	Collateral sesamoidean ligament
CL-DIP	Collateral ligament of the distal interphalangeal joint
TB	Thoroughbred
MSC	Mesenchymal stem cell
PRP	Platelet rich plasma
IGF-1	Insulin-like growth factor-1
PDGF	Platelet derived growth factor
VEGF	Vascular endothelial growth factor
bFGF	Basic fibroblast growth factor
TGF-β	Transforming growth factor beta
vWF	Von willebrands factor
MRI	Magnetic resonance imaging
STIR	Short tau inversion recovery
PD	Proton density
CT	Computed tomography
CECT	Contrast-enhanced computed tomography
JGB	Jennifer G. Barrett
LMG	Lauren M. Groom
MNA	M. Norris Adams
NAW	Nathaniel A. White II
EM	Elaine Meilahn

Overview of Thesis

Thesis organization

This thesis is presented in a format that contains a journal article as the central portion of the document. The publication is entitled, '*Accuracy of Open MRI for Guiding Injection of the Equine Deep Digital Flexor Tendon within the Hoof*' and contains its own introduction, materials and methods and discussion sections. The following introduction provides a brief summary of the research topic. The literature review will follow and provides an expanded summary of the pertinent background information about the topic. The final conclusions follow the manuscript, and suggest directions for future research. The references for both the literature review and manuscript are presented as one list at the end of the document.

Introduction

The foot is a common source of pain in horses and the deep digital flexor tendon (DDFT) is the most commonly injured soft-tissue structure within the foot. [1] Diagnosis of injury of the deep digital flexor tendon within the hoof is predominantly made by magnetic resonance imaging (MRI) and MRI studies have identified injury of the deep digital flexor tendon within the hoof as the primary cause of lameness in 10-43% of cases. [1-4] Studies show good correlation between low- and high-field MRI, and between lesion appearance and histopathology. [1, 5-7] Deep digital flexor tendon lesions are classified into 4 categories according to location and appearance on MRI: core lesions, parasagittal splits, dorsal abrasions and insertional lesions. [2] Lesions of the deep digital flexor tendon occur most commonly at the level of the navicular bone and proximal aspect of the navicular bursa and are typically confined to the medial or lateral lobe. [2, 8]

Treatment options for deep digital flexor tendinopathy are limited, consisting of long periods of stall rest with controlled hand walking and supportive shoeing. [1] The prognosis is poor, with only 25-28% of patients returning to previous levels of athletic performance. [1, 4, 9] Navicular bursoscopy is recommended to debride dorsal, intrabursal lesions, with 42% of patients returning to previous level of athletic performance. [10] Several alternative strategies have been used in the treatment of deep digital flexor tendon lesions, including intrabursal or intralesional injection of various biological therapies. [11-13] Experimental studies and limited clinical trials have shown

considerable promise in the use of intralesional biologic therapeutics for improving tendon healing. [11-14]

Due to the relative inaccessibility of the distal portion of the deep digital flexor tendon, intralesional injections have previously been performed with radiographic, [15] Computed Tomographic (CT)- [16], bursoscopic [17] or MRI- [18] guidance. The radiographic-guided injection technique allows for accurate injection of the deep digital flexor tendon on midline, at its insertion onto the distal phalanx. Currently, CT-, bursoscopic- and MRI-guided techniques to inject the distal deep digital flexor tendon require general anesthesia. Low-field, open MRI (Hallmarq Veterinary Imaging, Guildford, Surrey, UK) systems are becoming more available, with [19]s in use in equine clinics around the world. A major benefit of open MRI systems is that the exam can be performed with the horse standing with sedation rather than under general anesthesia. Core lesions that occur at the level of or just proximal to the navicular bone comprise the majority of targets for intralesional injection. MRI has been used extensively in human medicine to guide injection of various soft tissue structures. [20, 21] A standing, open MRI-guided injection technique of the deep digital flexor tendon has been used in 4 clinical cases in our hospital. Further investigation of this technique is warranted, as there are currently no validated methods available for injecting the distal portion of the deep digital flexor tendon in standing, sedated horses.

CHAPTER 1

Literature Review

Tendon composition, structure and biomechanical properties

Tendon composition

Tendons are a complex living tissue, with their main function being translation of muscular contractions into joint movement by transmitting forces from muscle to bone.[22] Tendons also store and release energy during the joint-loading cycle, which allows for more efficient movement; an important function of equine flexor tendons. Water is fundamental to the elastic properties of tendon, and makes up 66% of the total tissue weight. [23] The remainder consists of predominantly type I collagen (95% of total collagen), with smaller amounts of proteoglycans, glycoproteins and minor collagens, interspersed with tenocytes.[22] The remaining 5% of collagen consists of types III and V. Typically type III collagen is found in the endotenon and epitenon, but is also found in young tendon, injureed and healing tendon and ageing tendon; due to its smaller fibril size may result in decreased mechanical strength. Type V collagen is embedded in the core of type I collagen and regulates fibril growth. The proteoglycan content of tendon varies and depends on mechanical loading conditions, with small proteoglycans, such as decorin, predominating in tensile regions. [23] Decorin is located on the surface of collagen fibrils and is thought to facilitate fibrillar slippage during mechanical deformation. [24] Aggrecan, a large proteoglycan, holds water and resists compression, thus is increased in regions subjected to compressive forces. Glycoproteins, including fibronectin and tenascin-C, are also present in the extracellular matrix of tendons. [24] Tenascin-C is important for mechanical stability of the extracellular matrix through its interaction with collagen fibrils. Fibronectin is located on the surface of collagens and is thought to facilitate wound healing. Tendons also contain elastic fibers, which may contribute to the recovery of collagen crimp configuration after stretching. Tendon fibroblasts (also called tenocytes or tenoblasts) are the predominant cell type in tendons, and are aligned in parallel rows between fascicles. [25] They are responsible for synthesizing extracellular matrix proteins, producing an organized collagen matrix and remodeling during tendon healing. These cells have long cytoplasmic processes extending between collagen fibers,

which connect via gap junctions to produce a syncytium. This provides an efficient, three-dimensional network for mechanotransduction. [23]

One of the most abundant glycoproteins in tendons during growth is cartilage oligomatrix protein (COMP). [23] COMP, or thrombospondin, has a pentameric structure that allows for high binding affinity with collagens type III and I. [26] COMP is involved in arranging collagen molecules in the typical quarter-stagger array, and thus is important in collagen fibrillogenesis. Equine studies have shown that COMP levels are universally low in all tendons at birth, and then increase exponentially with age to peak at around 2 years of age in flexor tendons. [27] The tensional regions peak at around twice the level of compressed regions, and then decline rapidly, while levels are maintained in compressed regions during maturity. In contrast, COMP levels in extensor tendons remain essentially constant at a low level. Furthermore, there has been a positive correlation found between ultimate tensile stress and COMP levels, suggesting that this is an important protein in the development of strong tendons. [27] It has been suggested that the higher the COMP level during growth, the stronger the resulting tendons, thus promoting COMP synthesis during growth would potentially improve tendon quality and reduce the risk of tendinopathy.

Tendon structure

Collagen is synthesized as α-helical chains with amino- and carboxy-terminal extensions. [25] These are cleaved by procollagenases before three α-chains are combined into a triple helix configuration to form a collagen molecule. Aggregates of collagen molecules are held together by cross-links (microfibers). Cross-linking increases Young's modulus and reduces strain at failure. [24] The collagen fibril is the smallest structural unit of the tendon, made up of collagen molecules aligned end-to-end in a quarter-stagger array (Figure 1). [24] Fibril diameters vary from 10-500nm, with younger animals typically having small fibrils and mature animals having a combination of small and large fibrils. [24] When unloaded the fibrils have a 'crimped' appearance, which allows the fibril to function as a biological spring; opening with tension and recoiling with unloading. [23] Collagen fibril size has been correlated with tendon stiffness, with larger fibrils resulting in a stiffer tissue. In adult tendons, differences in fibril size exist between tendons with different functions; the deep digital flexor tendon has fewer small-diameter and more large-

diameter fibers compared to the superficial digital flexor tendon. The next largest structures in tendons are fibers, formed by bundles of collagen fibrils separated by cytoplasmic extensions of tenocytes. [25] The fibers are then bundled into fascicles, bound by endotenon, a thin layer of connective tissue, which contains blood vessel, nerves and lymphatics. The overall tendon unit is made up of many fascicles bound by epitenon, a loose connective tissue layer containing the neurovascular supply to the tendon. When not enclosed by a synovial sheath, a denser connective tissue layer, paratenon, surrounds the tendon to reduce friction with adjacent tissue. The vascular supply to tendons arises form the muscular origin, osseous insertion and from mesotenon attachments. [25]

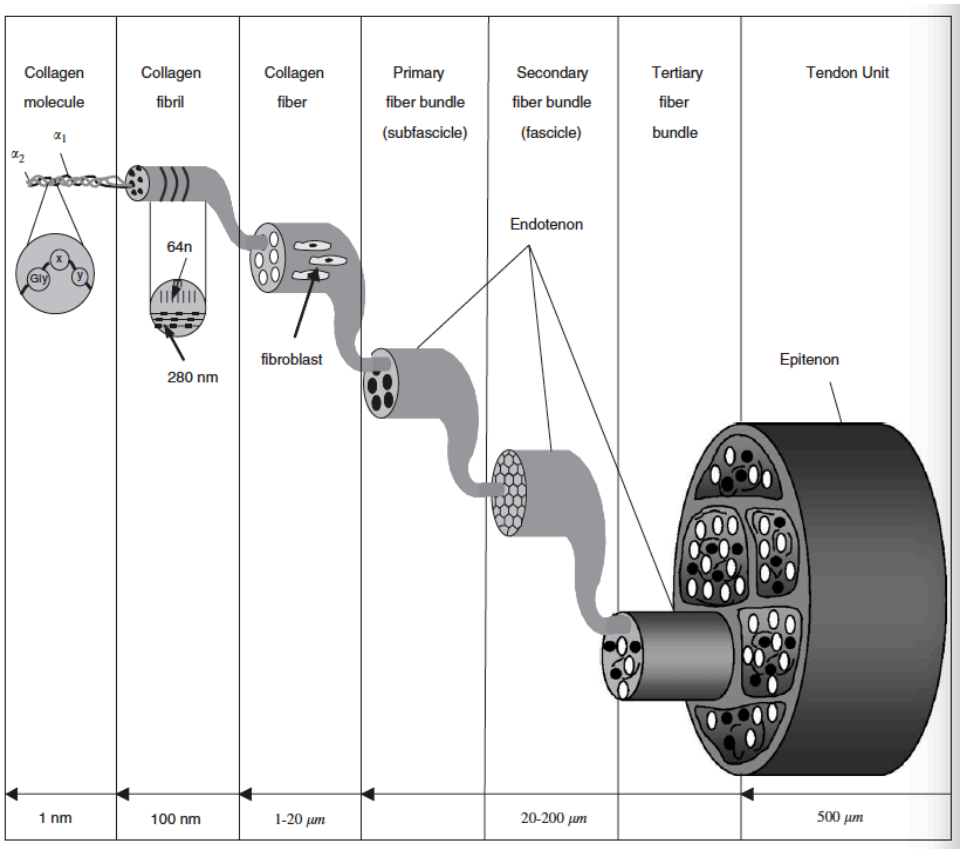

Figure 1. Tendon structure. [24i]

[i] Reprinted from the Journal of Biomechanics, Wang, H.C., Mechanobiology of tendon, 1563-1582, Copyright (2006), with permission from Wange, H.C. and the Journal of Biomechanics.

Tendon biomechanics

The biomechanical properties of tendons can be defined *in vitro* by their structural and material properties. [23] Tendon loading experiments that load a sample to failure generate a load-deformation curve, which determines ultimate tensile strength and stiffness (Figure 2). Then, if the tendon's cross-sectional area and length are known, stress can be plotted against strain to determine ultimate tensile stress and Young's modulus of elasticity. Stress is defined as force per unit area [i]and strain as change in length over the original length.

When tendon is loaded initially during the 'toe' region, collagen fiber crimp elongates resulting in relatively greater stretch for lower loads. [25] After this the stress-strain relationship becomes linear, with collagen fibers sliding relative to each other. The slope of this portion of the curve is known as Young's modulus and represents the stiffness of the tendon. At the tendon's yield point, the gradient changes as covalent crosslinks rupture and irreversible slippage of collagen fibers occurs. If loading is continued beyond this point, macroscopic failure occurs as the tendon ruptures. The ultimate tensile strain reflects the final strain before rupture occurs. Equine superficial digital flexor tendon has a reported ultimate tensile strain of 25% *in vitro*. [23] *In vivo* experiments have shown a strain of 16.6% occurs in the SDFT at a gallop, thus there is little tolerance for deterioration in mechanical properties before injury occurs.

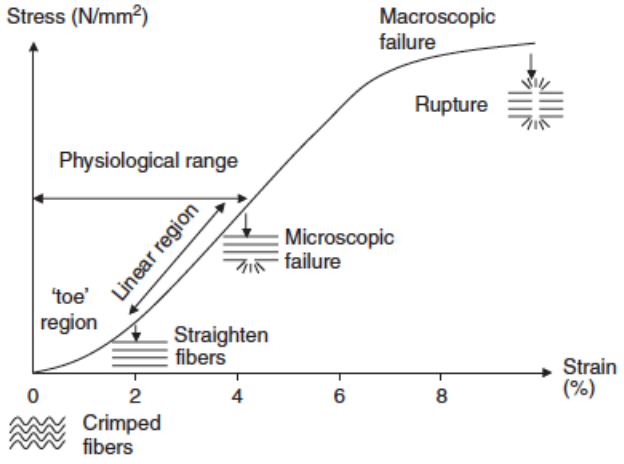

Figure 2. The stress-strain curve. [24i]

[i] Reprinted from the Journal of Biomechanics, Wang, H.C., Mechanobiology of tendon, 1563-1582, Copyright (2006), with permission from Wange, H.C. and the Journal of Biomechanics.

Tendons have viscoelastic properties, meaning their mechanical properties vary in response to mechanical loading. A component of this, termed hysteresis, is shown by the differences in the stress-strain relationship between loaded and unloaded tendon (Figure 3). [23] The area between the two curves represents energy lost during the loading cycle, most of which is lost as heat. In equine tendons, this is usually around 5%, and is responsible for the rise in core temperature in tendons during exercise.

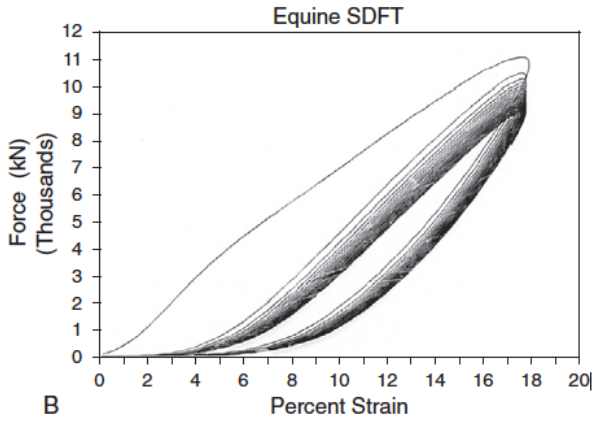

Figure 3: The hysteresis loop: loading and unloading curves are not overlapping due to energy loss during unloading. This energy equals the area between the two curves. With repeated loading, the curve moves to the right as the tendon becomes more elastic. [25i]

Due to their viscoelastic properties loading rate affects tendon properties, with tendons being more deformable at low strain rates. [23] Thus more rapid loading (high strain rate) results in relatively increased stiffness. This concept is important when examining the function of tendons, in particular the equine flexor tendons. The horse has evolved a number of mechanisms to allow for high speed, efficient locomotion. The distal limb is elongated and reduced to a single digit, with musculature positioned in the proximal limb. The palmar soft tissues act as an elastic unit to store energy allowing for efficient locomotion. The energy stored is represented by the area under the stress-strain curve, and is returned during the protraction phase with an efficiency of 93%. [23] Tendon-specific differences are seen in composition and material properties based on

[i]Reprinted from the Equine Surgery, Auer, J.A. and Stick, J.A., Chapter 83- Diagnosis and Management of Tendon and Ligament Disorders, ed. Avella, C.S and Smith, R.K. W., Copyright (2012), with permission from Elsevier Inc.

their function. For example, the superficial digital flexor tendon, highly important in storing energy has an entirely different function compared to the common digital extensor tendon. The SDFT has a lower elastic modulus and ultimate tensile stress than the CDET but the strain at peak stress is greater in the SDFT. On a molecular level, the SDFT has a higher water and glycosaminoglycan (GAG) content and higher cellularity than the CDET. In addition, the SDFT has a significant rise in COMP levels after birth, which does not occur in the CDET.

Changes with age and exercise

The structure and biomechemical properties of tendons are influenced by training and age. As mentioned, the COMP profile of tendons changes with age, being low at birth and peaking in the tensile region of the flexor tendons at around 2 years of age. At this time, collagen fibrils undergo maturational change including decreased crimp angle and length, increased mature crosslinks and decreased reducible crosslinks and increases in the average collagen fibril diameter. [28] It appears that tendons at birth are homogenous throughout their length, and that site-specific variations related to external compressive forces develop after birth. [29] Therefore, appropriate external stimuli are likely necessary to stimulate optimal tendon development. Animal studies have shown an increase in number and size of collagen fibrils and higher ultimate load and energy absorbed after training. [24] There is also an overall decrease in collagen maturation in tendons following strenuous activity due to an increase in collagen. Equine studies in immature animals have shown differences in tendon strength and structure with varying exercise regimes. In one study, foals kept at pasture had significantly stronger tendons at five months of age *versus* those kept in a stall and exercised on a treadmill. [30] The stall confinement with treadmill group also had lower COMP and polysulphated GAGs, suggesting activity affects tendon development. Interestingly, after all animals were returned to free pasture exercise from age 5-11 months, there was some recovery in tendon properties. This suggests that there may be an early 'window of opportunity' for tendon adaptation. It has been suggested that equine flexor tendons lose their ability to adapt to exercise after skeletal maturity and that both ageing and excess exercise provoke tendon degeneration. [23] The association between age and exercise suggests that number of loading cycles is important in tendon degeneration, and it is likely that higher loading rates (galloping) are the most damaging. It has been shown that older horses are more likely to develop tendinopathy, with TB racehorses > 5 years old having a 15 times

increased risk of SDFT injury than 2 year old horses in one study. [31] Changes reported in equine SDFT associated with gallop exercise include changes in collagen crimp morphology, decreased collagen fibril diameter, accumulation of partially degraded collagen and a reduction in glycosaminoglycan content. [32, 33] This suggests that the susceptibility of older individuals to tendinopathy may be due to an inability to remove partially degraded collagen from the matrix resulting in decreased mechanical competence. The precise mechanism for tendon degeneration is not known, but may include either physical or metabolic processes. [23] Physical energy imparted during weight bearing can cause direct damage to tendon matrix and indirectly through hysteresis. Cell mediated processes such as the release of proteolytic enzymes may also be involved.

Tendon injury and repair

Tendon healing follows a similar progression of three overlapping phases as other tissues. The initial inflammatory stage, lasting 24-48 hours, involves infiltration of red blood cells, platelets and inflammatory cells to the site of injury. [22, 24] A fibrin clot is formed and macrophages phagocytose necrotic material. IGF-1 is expressed during the early inflammatory phase to recruit fibroblasts leading to collagen and proteoglycan production. After 48 hours, and peaking at 3-6 weeks, the reparative phase begins. [24, 34] This phase is characterized by synthetic activity with fibroblasts producing abundant collagen and other extracellular matrix products at the injured site. The morphology of these fibroblasts is different to normal tenocytes, being larger and more basophilic with large nuclei similar to myofibroblasts. [35] Macrophages shift from a phagocytic to reparative role, releasing growth factors for cell recruitment. There are five main growth factors that are important in tendon healing; insulin-like growth factor-1 (IGF-1), platelet-derived growth factor (PDGF), vascular endothelial growth factor (VEGF), basic fibroblast growth factor (bFGF) and transforming growth factor-beta (TGF-β). [24] VEGF is important in stimulating endothelial cell proliferation, angiogenesis and increasing capillary permeability. During this phase, the water and GAG tissue content are high and the matrix consists of increased collagen type III with less cross-links than normal tendon. [35] Type III collagen has smaller fiber size than type I, which results in reduced strength. The remodeling phase begins around 8-12 weeks following injury and results in a change to fibrous then fibrotic, poorly organized tendon tissue. There is a shift to collagen type I and decreased cellularity and GAG synthesis. In the last part of

this phase, covalent bonds between collagen fibers increases resulting in increased tensile strength and stiffness; however, the repair tissue has inferior biomechanical properties than before injury due to deficient structural and matrix composition. [35] This increased stiffness reduces elasticity and thus function of the tendon as a spring. Loading should be minimized during the early inflammatory phase to avoid disrupting the healing process, however, controlled mobilization after the first week has been shown to enhance the quality of healing tendons. [24] Mobilization stimulates tenoblasts which respond by altering gene expression, protein synthesis and cell phenotype. This results in fibroblast proliferation, increased collagen synthesis and release of growth factors, which ultimately leads to stronger tendons with fewer adhesions.

Tendinopathy

It has been well established that typically, before clinical evidence of tendon injury, there is a period of subclinical pathology resulting from cumulative microdamage. [36] This does not preclude the acute rupture of a healthy tendon due to overwhelming mechanical loads, which is less common. [32] There may be a continuum of pathologic change that ranges from failure of adaptation to exercise, through progressive stages of proliferative reaction, disrepair and degeneration leading to a potentially irreversible state. [37] Observations made in the literature support the idea that preceding degeneration occurs in tendinopathy including the identification of 'asymptomatic' lesions in post-mortem studies, the bilateral presentation of many tendinopathy's with one limb more severely affected and the close epidemiological association between age, exercise and tendon injury. [23] It is unknown exactly why tenocytes fail to repair exercise-induced microdamage, but may involve reduced cell numbers and gap junctions, absent growth factor stimulus and a degree of cellular senescence. [25] In the acute stage of injury, when macroscale damage occurs resulting in clinical disease, overt signs of inflammation (heat, pain swelling) are present. However, this acute phase is short and signs of inflammation are typically not present during the chronic phase of injury. Thus, the role of inflammation in tendinopathy is controversial in the literature. Overstrain tendon injuries in humans and equine subjects are thought to be primarily degenerative due to the lack of obvious signs of inflammation, hence the term tendinopathy *versus* tendonitis. [34] However, this absence of clinically evident inflammation does not preclude a primary role for inflammatory mediators during pathogenesis and healing of tendon lesions at the cellular level.

Much of the research in tendinopathy has been performed in equine superficial digital flexor tendons due to strong similarities in function, structure and injury to the human Achilles tendon. Early stage equine SDFT tendinopathy is characterized by increased cellularity and on examination of these cells, macrophages with a pro-inflammatory phenotype are abundant. [36] In the later stages of healing there is a transition to anti-inflammatory/pro-fibrotic phenotypes. The resolution of inflammation has been shown to be highly regulated and active, with specific 'pro-resolving mediators' activating endogenous stop signals for inflammation. [34] Key events in the resolution of inflammation include phagocytosis of apoptotic cells, modification of the inflammatory cell infiltration and vascular changes. When this system fails or there is a persistent inflammatory stimulus with chronic inflammation, the end result is fibrosis. [36]

Fibrosis is defined by scarring of tissues due to excessive deposition of extracellular matrix components such as proteoglycans, GAGs and collagen type III. Fibrotic tissue is biomechanically inferior to elastic tendon tissue and is prone to recurrent injury, especially at the interface of normal and injured tissue. [23] Blocking inflammation has been shown to stop activation of pathways that assist in resolution of the injury. [34] Therefore, from a therapeutic approach, it is important to moderate inflammation while potentiating resolution, rather than widespread or complete inhibition of inflammatory processes. Furthermore, increased age has been shown to reduce the ability to respond to inflammation. An equine study showed an age-associated decreased in expression of an inflammation-resolving protein (FRP2/ALX) in injured equine SDFTs. [38] Thus, ageing is another suggested mechanism for the development of chronic inflammation and re-injury.

Equine DDF tendinopathy

DDFT anatomy and function

Most experimental work on tendinopathy has focused on the equine superficial digital flexor tendon. The equine deep digital flexor tendon is different in function and has minor differences in composition compared to the superficial digital flexor tendon, therefore pathogenesis of injury and healing may not be the same. In the forelimb, the deep digital flexor muscle consists of three heads; the humeral, ulnar and radial. [39] These three muscle bellies form tendons which unite at

the level of the radiocarpal joint and form a broad, triangular shape tendon that progresses through the carpal canal. In the middle metacarpus, then tendon is joined by its accessory ligament, arising from the palmar carpal ligament and proximal third metacarpal bone. Proximal to the fetlock, the DDFT is enclosed by the manica flexoria of the SDFT, with both structures traveling through the digital flexor tendon sheath. In the pastern, the DDFT forms two rounded, symmetrical lobes. The dimensions are narrowest in the proximal pastern, where the DDFT passes between the distal SDFT branches, after which it increases in size, in both the dorsopalmar and lateromedial plane. Within the foot, the DDFT dorsal surface lies within the navicular bursa and this surface contour mirrors the palmar aspect of the navicular bone. At the distal margin of the navicular bone, the direction of the tendon angulates dorsally and becomes fan-like, inserting on the facies flexoria of the distal phalanx, between the medial and lateral palmar processes. [40]

During the first part of stance phase in the forelimb, the DDFT is only in contact with the distal palmar border of the navicular bone (distal interphalangeal joint flexion). [39] During the propulsion phase, the DDFT undergoes a relative distal sliding and comes into full contact with the palmar surface of the navicular bone. Thus, the distal scutum acts as a lever to facilitate foot rotation and heel takeoff at the end of the stance phase. It is during this phase that the DDFT is under maximum tension and most susceptible to injury. The DDFT has an important role in stabilizing the distal interphalangeal joint by compressing the dorsal articular surface of the navicular bone against the palmar articular surfaces of the middle and distal phalanges. [41] Similar, but to less of a degree than the SDFT, tension induced in the DDFT during weight bearing leads to flexion of the interphalangeal, metacarpophalangeal and carpal joints during the following swing phase. The dorsal 20-30% of the tendon is specialized just proximal to the navicular bursa, with a fibrocartilage zone rich in elastic fibers. [42] This is thought to be a functional adaptation to compressive loading and is analogous to the fibrocartilaginous portion of the SDFT palmar the metacarpophalangeal joint. [41] Similarly, at the level of the fetlock the DDFT has mixed fibrocartilaginous architecture, with chondrocytes interspersed between collagen fibers.

The DDFT has its vascular supply from three main sources in the forelimb. [39] Proximal to the fetlock, the common digital artery gives off a distal metacarpal branch at the palmar aspect of the tendon. Distal to the fetlock, vessels arising from the palmar branches of the proximal phalanx supply a dorsal sagittal artery to the dorsal tendon. The terminal DDFT is supplied by two small vessels on either side, which arise from the proper digital artery. There is an extensive vascular network within the DDFT, except for the palmar aspect of the fetlock where there is variable amounts of fibrocartilage. In the foot, the dorsal parts of the tendon are more poorly vascularized than the palmar regions.

Pathophysiology

The etiopathogenesis of digital DDF tendinopathy is not completely understood. Multiple studies have been performed comparing the MRI findings and histopathology of horses with lameness localized to the palmar foot *versus* non-lame control horses. [5, 40, 42, 43] A common change associated with DDFT pathology in lame horses are adhesions, either between the DDFT and collateral sesamoidean ligament or DDFT to distal sesamoidean impar ligament. There is good correlation between MRI diagnosis of adhesion formation and the identification of adhesions on gross examination. [40]

Histopathologically, core lesions consist of varying amounts of collagen necrosis, fibroplasia and fibrocartilaginous metaplasia, which disrupts normal fascicular architecture. In one study, lesions from horses with lameness between 2-6 months duration had necrotic core lesions, whereas those from horses with lameness of > 6 months duration had core fibroplasia and fibrocartilaginous metaplasia. In close proximity to these lesions there is typically thickening of interfasicular septae with evidence of proteoglycan accumulation, and vascular changes including blood vessel ghosting and occlusion. Core necrosis is more common in the deep dorsal area of the tendon and is characterized by areas of coalescing pseudocystic spaces containing basophilic and eosinophilic breakdown material. [40] There can also be evidence of revascularization in the periphery of these lesions in some cases. At the level of the navicular bone, lesions consist of interfascicular septal and fascicular fibrocartilaginous metaplasia with prominent groups of occluded interfascicular blood vessels. Dorsal splitting is also seen at this

level, with the more severe, deeper splits occurring in horses with lameness < 6 months duration. [40] When pathology is associated with the deep dorsal layer of the DDFT at the level of the navicular bone and insertion, there is often evidence of revascularization.

In a histopathological study of DDFT lesions, the normal, control limbs showed some evidence of degenerative changes including thickened interfascicular septa, sometimes with cartilaginous metaplasia, vascular changes and septal proteoglycan deposition. [40] This suggests that microstructural changes to the interstitial matrix can occur without production of pain, and may represent early degenerative changes. A finding that has been common among all histopathological studies of equine distal DDFT injury is a lack of inflammation. Busoni *et al.* (2005) [5] suggested that the term tendinopathy should be used instead of tendonitis to describe distal DDFT injury due to the lack of histological signs of inflammation. There has also been a strong correlation shown between distal DDFT injury and navicular bone disease, and it is suspected that lesions may be part of the same degenerative complex. [42] A limitation of these studies is that the cases were all chronic or severe, and most were lame for at least 2 months, or had severe enough disease to result in radiographic signs of navicular syndrome. This suggests that cases were not seen in the acute or sub-acute phase of injury, which may account for the lack of evidence of inflammation. Furthermore, in most series, only three sections (one from each level) of tendon were examined, so lesions may have been missed. At this stage, the role of inflammation in the progression of these chronic lesions is not known.

Another finding across multiple large histopathological studies is the increased presence of vascular changes in the DDFT in horses with foot pain compared to age-matched control horses. [5, 7, 40, 42] Changes include vessel occlusion and blood vessel ghosting, as well as evidence of revascularization associated with dorsal and core lesions. [40] Vascular compromise may result in matrix changes that predispose the horse to injury of the distal DDFT. Matrix changes associated with ageing have also been suggested to play a role in tendon degeneration. Studies have found increased volume of collagen, decreased fibroblast cellularity and metabolism and an associated loss of proteoglycan with ageing DDFTs. [44, 45] Special stains and immunohistochemistry have been used to provide further evidence for differences between horses with chronic foot pain and age-matched controls. [46] Beck *et al.* (2011) found increased neovascularization and proteoglycan

staining intensity in the distal DDFT of horses with chronic foot pain. Neovascularization has been associated with chronic human Achilles tendinopathy and is suspected to indicate pathological change. [46] Tendons adapt to stress with proteoglycan deposition, so increased levels may be an indicator of degeneration. Immunohistochemistry staining for Factor VIII and von Willebrands Factor (vWF) (markers for endothelial cell function and vascular viability) revealed a higher frequency of vascular injury in the chronic lameness group, which may have stimulated vascular proliferation.

The anatomical adaption of the distal DDFT, with a prominent zone of fibrocartilage at the level of the distal interphalangeal joint is a typical modification seen in tendons at sites of increased loading. Histological studies confirm this region to be relatively avascular, with the deep dorsal and palmar regions having greater vascularity. [40, 47] The poor vascularity of this zone, combined with strenuous exercise could compromise vascular perfusion to the foot and create a period of hypoxia. Fibrocartilaginous metaplasia can occur with hypoxic conditions, therefore any vascular compromise in a tendon subjected to considerable loads may induce matrix changes as seen in pathological studies. [40] The resulting changes further reduce vascularization by proteoglycan deposition around blood vessels, which contributes to a cycle of degeneration.

Incidence

The foot is a common source of pain in horses, especially in front limbs [48]. In the past decade, advances in diagnostic imaging have revealed that DDFT is the most commonly injured soft-tissue structure within the foot [1]. The reported incidence of DDFT lesions in both low- and high-field MRI series ranges from 21%- 83%, depending on the study. [1-3, 6, 8, 49, 50] The incidence of DDFT lesions being the primary cause of pain is 10-43%. [1-4] Tendinopathy of the DDFT may occur alone, in conjunction with navicular bone injury or in association with multiple soft-tissue injuries within the foot. [1, 3]

Lesions of the DDFT most commonly occur at the level of the navicular bone and proximal aspect of the navicular bursa. [3, 8] The frequency of lesion type at different locations varies, with core lesions predominating at the level of the proximal interphalangeal joint (43%) and proximal phalanx (>90%). [8] At the level of the navicular bone, parasagittal splits (31-81%) and dorsal

abrasions (59%) are most common, followed by core lesions (19-25%).[3, 4, 8] At the proximal aspect of the navicular bursa, dorsal abrasions (71%) are most common, followed by parasagittal splits (13-29%) and core lesions (23-35%). Distal to the navicular bone, lesions are more difficult to classify, but consist of core lesions (74%), dorsal abrasions (51%) and parasagittal lesions (26%).

Multifocal lesions are reported to occur in 17-43% of cases.[1, 3] In case series of lesions in one limb, [3] 84% of DDFT lesions occurred proximal to the navicular bone. In case series which reports DDFT tendinopathy as the primary source of pain, there were concurrent lesions of the podotrochlear apparatus reported in 67% of cases. [4] Navicular bone abnormalities are most common and include flexor cortex erosions, distal border fragmentation, signal changes in the medulla and thickening of the palmar cortex. [51]

Other concurrent pathologies include desmitis of the collateral ligaments of the distal interphalangeal joint, collateral sesamoidean ligament (CSL) or distal impar sesamoidean ligament (DSIL). Adhesions between the DDFT and navicular bone, collateral sesamoidean ligament or distal impar sesamoidean ligament also commonly occur while concurrent osteoarthritis of the distal interphalangeal joint is less common. Non-specific findings of effusion in the coffin joint and/or navicular bursa are also common. A correlation has been seen with lesions of the DSIL and CSL and increased signal of the medulla of the navicular bone, with more chronic cases having enthesophyte formation and distal border fragmentation. [8] These injuries may reflect the line of stress of the podotrochlear apparatus during weight bearing. An association has also been seen between DDFT dorsal abrasions and sagittal splits and flexor cortex lesions of the navicular bone. It is thought that these tendon lesions may predispose to lesions of the navicular bone cartilage. [8, 51] While dorsal abrasions typically occur with concurrent navicular bone disease, core lesions tend to occur independent from navicular bone abnormalities.[41, 51] Thus, it may be possible that a different etiology exists for primary DDFT lesions compared to those that occur in association with navicular disease.

DDFT lesions are classified into 4 categories according to their MRI appearance: core lesions, parasagittal splits, dorsal abrasions and insertional lesions.[8] Core lesions appear as focal, round

areas of hyperintense signal in the central or dorsal portion of the affected lobe, and are surrounded by normal, hypointense tendon.[41] They average 45mm in length, ranging from 5 to 135mm.[42] In one MRI series, core lesions had increased signal intensity in T1-, T2-weighted sequences and fat suppressed images in 90% of cases lame for < 6 months and in only 20% of cases lame for > 6 months. Furthermore, 92% of core lesions with core necrosis had increased signal in fat suppressed images compared to no core lesions consisting of fibrosis and fibrocartilaginous metaplasia. This suggests that appearance on different MRI sequences correlates with histopathology and chronicity of lesions. Parasagittal splits form linear hyperintensities, which arise from the dorsal border and extend to a variable depth along septal lines.[4] Dorsal abrasions occur at the level of the navicular bone, and range from mild irregularities of the dorsal border to signal hyperintensities that extend towards the center of the affected lobe. [8] Insertional lesions refer to short parasagittal splits or core lesions, which extend <20mm from the insertion of the DDFT on the distal phalanx.

Risk factors for DDFT injury include jumping disciplines, abnormal angle of the DDFT as it passes over the distal phalanx, hoof conformation and previous palmar digital neurectomy.[41, 52] These injuries may be the result of acute traumatic overload at the end of the stance phase, or due to repetitive overload stress. It has been found through theoretical modeling that for every one-degree increase in the palmar angle of the distal phalanx, there is a 4% increase in peak force exerted by the DDFT on the navicular bone at the end of the stance phase. [53] Clinical studies have evaluated this concept further, with McCormick *et al.* showing that the angle of the DDFT as it passed over the navicular bone was significantly more acute in horses with DDFT lesions compared to controls. [52] Another study failed to show a significant association, but did find a trend in Thoroughbreds with DDFT lesions to have more acute distal phalanx angles than clinically sound Thoroughbreds. [54] The significance of these findings is not known, but may suggest that increased DDFT loading with more acute angulation predisposes to injury, supporting the theory of repetitive overload stress. Another known risk factor for DDF tendinopathy is jumping, with the risk increasing proportionally with height and intensity of the jumps. [2, 6] This also provides support for the theory of overload injury.

Diagnosis of DDF tendinopathy

Clinical examination

DDFT tendinopathy typically causes lameness in mature horses, 5-14 years of age. [48] The lameness may be acute in onset and moderate-severe in nature or can present as a more insidious, chronic lameness. Historically, horses that became sound after diagnostic analgesia of the palmar/plantar digital nerves without other radiographic abnormalities were considered to have navicular syndrome. [1] Increased availability of advanced imaging over the past two decades has revealed a high incidence of primary soft tissue injury responding to this nerve block. A pattern of diagnostic analgesia has emerged through the study of large numbers of clinical cases. Seventy-two percent of horses with either primary DDFT or collateral ligament of the distal interphalangeal joint (CL-DIP) injury will improve >50% after diagnostic analgesia of the palmar/plantar digital nerves. [2, 55] In contrast, 68% of horses with DDFT and only 24% of horses with primary CL-DIP injury improve with intra-articular analgesia of the DIP.

Intra-thecal analgesia of the navicular bursa resulted in 62% of horses with primary DDFT improving, compared to none of the horses with primary CL-DIP injury. Intra-thecal analgesia of the digital flexor tendon sheath may also improve lameness in horses with primary DDFT injury. However, overall complete resolution of lameness is achieved following these blocks in only 20% of horses, with an abaxial nerve block required to abolish lameness. Furthermore, other structures such as the navicular bone and distal interphalangeal joint are also affected by these nerve blocks and there is a high incidence of concurrent bone pathology with soft tissue injury to the foot. [41] In one case series, a trend was found for increased lameness in a straight line associated with parasagittal splits compared to dorsal border and core lesions. [56] These authors also compared cases with repeat MRI examination at 3 and 6 months following conservative treatment, and no correlation was found with signal intensity and lameness score.

Diagnostic imaging

Due to limitaitons of ultrasonographic imaging of soft tissues within the hoof, diagnosis of injury to the distal portion of the DDFT is predominately an MRI diagnosis. Radiographs of horses with distal DDFT tendinopathy are usually normal, unless concurrent navicular bone pathology exists. Occasionally, focal osteolysis and surrounding sclerosis may be seen in the facies flexoria of the

distal phalanx with severe cases of enthesopathy. [41] Also, when significant radiographic abnormalities of the flexor surface of the navicular bone are present, there is likely concurrent erosive damage to the dorsal surface of the DDFT.

Ultrasonography has been used to image the DDFT as far distally as the proximal border of the navicular bone with a microconvex ultrasound probe [57]. At the level of P2, the tendon must be imaged at a more acute angle than the normal 90º due to an inability to position the transducer perpendicular to the DDFT creating an off-incidence angle artifact. The margins and symmetry of both lobes can typically be evaluated, but fiber damage and alignment cannot be assessed. [58] Horses with upright, contracted heels are more challenging and imaging at this level may not be possible. Findings that may be identified with injury include dorsal bulging, lobe symmetry and hyperechoic areas consistent with mineralization. A transcuneal approach has also been described, however, the field of view is limited to the central third of the tendon at the navicular bone and off-incidence angle artifacts are common. [58] The ability for ultrasonography to detect DDFT lesions compared with MRI ranges from 10%- 28%, so this imaging modality is not as useful in the diagnosis of foot-related problems.[2, 6, 58]

Distal DDF tendinopathy has been associated with focally increased radiopharmaceutical uptake in the region of the DDFT during soft tissue-phase nuclear scintigraphy. [59] Bone phase imaging may also reveal increased radiopharmaceutical uptake in the region of the DDFT insertion on the facies flexoria of the distal phalanx, due to abnormal bone remodeling secondary to enthesophathy. Abnormalities of the navicular bone commonly lead to increased radiopharmaceutical uptake on nuclear scintigraphy and must be distinguished from soft-tissue injuries. [60] In one cases series, scintigraphic abnormalities were found in 40% of horses with distal DDFT tendinopathy, and were more common when the lameness duration is > 3 months. [2] In another study, there was over-representation of higher scintigraphy grades for DDFT lesions at the level of the navicular bone, proximal interphalangeal joint and DSIL, suggesting lesions at these locations have a relationship with lesions of the navicular bone. [59] The sensitivity of nuclear scintigraphy for distal DDFT tendinopathy is reportedly low; however, the specificity is relatively good for soft-tissue phase images. [2] This suggests that while nuclear scintigraphy does

not rule out DDFT tendinopathy in the foot, positive radiopharmaceutical uptake is a good predictor and further diagnostic imaging should be used in these cases.

Advanced imaging

Diagnosis of distal DDF tendinopathy in the horse's foot is typically made using magnetic resonance imaging. To understand the value and limitations of MRI, a brief review of MRI physics is warranted. Magnetic resonance imaging has unique characteristics related to the underlying physics behind signal generation and image formation. In the presence of a magnetic field, certain protons (predominately hydrogen) in the body become sensitive and will resonate in a synchronized matter, with the frequency of magnetic oscillations at which the nuclei resonate being proportional to the strength of the magnetic field. [61] The protons align either parallel or anti-parallel with the magnetic field, with more aligning in the parallel state. Thus there is a net magnetic moment aligned with or longitudinal to the magnetic field. The protons 'precess', with the precession frequency dependent on the strength of the external magnetic field. [62] A radiofrequency pulse with the same frequency as the processing protons can be applied and causes resonance, or transfer of energy between the protons, causing the protons to precess in sync with a new net magnetic moment aligned transverse to the magnetic field. After switching off the RF pulse, longitudinal magnetization increases as the net magnetization re-aligns parallel with the external field; this is described by a time constant, the T1 or longitudinal relaxation time. [62] Also after switching off the RF pulse, the transverse magnetization decreases due to loss of phase coherence and disappears; this is also described by a time constant, the T2 or transverse relaxation time. The relaxation times between various tissues are different which can be used to distinguish between tissue types. Overall, T1 is longer than T2 and varies with the magnetic field strength, being longer in a stronger magnetic field. Typically, water has a long T1 and T2 and fat has a short T1. [62]

Magnetic resonance imaging allows for the creation and detection of signals using the H protons in fat and water. [61] By applying a linear magnetic field gradient, the position of the resonating nuclei within the body can be determined. To measure the position in three-dimensions, a succession of field gradients are applied. Pulse sequences involve the application of one or more RF pulses, switching on/off field gradients in all three directions and the acquisition of the

resulting RF signal. The time between pulse sequences, repetition time (TR) will determine how much T1 or T2 properties influence the signal obtained. [62] For example, if the TR is long, all tissues will have regained their longitudinal magnetization by the time the second RF pulse occurs; therefore, the transverse magnetization after the second pulse will be the same as after the first pulse. If the time is short, however, tissue A may have regained more longitudinal magnetization than tissue B (due to T1 properties); therefore, when the second RF pulse hits, the transverse magnetization of tissue A is larger thus a different signal intensity will be produced. Therefore, the differences is signal intensity between tissues when using a short TR is determined by differences in their T1 properties, therefore this is called a T1-weighted image. If a 180° RF pulse is applied a certain period after the initial 90° RF pulse, the precessing protons spin in the opposite direction creating a strong signal called a spin echo. [62] The time between the original 90° pulse and the spin echo is called the time to echo (TE). With multiple 180° pulses, the signal decrease between echos is due to T2 effects. If the TE is short, a strong signal is obtained; however, differences in T2 properties are not yet seen between tissues. The longer the TE, the greater the differences will be in T2 properties between tissues. However, waiting too long results in low signal intensity which results in a grainy image. The TR and TE can be chosen when planning pulse sequences to manipulate the resulting signals. When a long TR is chosen, T1 differences have no effect on signal. When a short TE is chosen, differences due to T2 properties have not had time to have effect. Therefore, with a long TR and short TE, differences in signal intensity are influenced by proton density, with more protons resulting in greater signal. Paramagnetic substances such as gadopentetate dimeglumine (Magnevist, Bayer Health Care LLC, USA) shorten T1 and T2 of the surrounding protons which results in a signal increase in T1-weighted and signal decrease in T2-weighted images.

The two basic pulse sequences are gradient echo and spin echo. [61] Spin echo sequences are composed of a 90° then 180° pulse. [62] A problem with the spin echo is that using the 180° pulse is time consuming. Therefore in gradient echo sequences, instead of the 180° pulse a magnetic field gradient is applied for a short time which results in greater magnetic field inhomogeneities. Subsequently, transverse magnetization occurs faster and the gradient is applied again to refocus the dephasing protons again, producing a signal called a gradient echo. TR also affects speed of imaging, so ideally a short TR results in a faster scan, however, this results in a small amount of

longitudinal magnetization. To overcome this, pulses that cause a small flip angle of around 10-35° are used so that the longitudinal magnetization is not completely abolished. Due to the use of a magnetic gradient instead of a 180° pulse, signal intensity decays faster which is due to T2* effects. Larger flip angles >30 degrees can be used to show T1 effects.

Another sequence type used commonly is an inversion recovery sequence. [61] A 180° pulse is applied first, followed by a spin echo sequences. The inversion time (TI) is the time between the 180° and 90° pulse. The inversion time can be selected to suppress signal from certain tissue types. For example, a STIR (short tau inversion recovery) sequences is used to suppress fat signal and increase the ability to detect water, which is very useful to detect signs of imflammation in tissues.

The strength of an MRI signal increases in proportion to the strength of the magnet, which has a strong influence on image quality. [61] MRI units are defined by their field strength as low field (up to 0.3T) or high field (1-1.5T or higher). [63] The lower cost of low-field systems has increased availability in the equine market. As of 2016, there are 87 low-field units made by Hallmarq Veterinary Imaging with an open magnet configuration that allows imaging of the limbs of horses that are sedated and standing rather than under general anesthesia. Differences between low- and high-field systems influence spatial resolution, contrast resolution and noise. Images acquired with low-field systems have longer acquisition times resulting in motion artefacts. Therefore, the faster acquisition times of gradient echo sequences are advantageous. [63] However, these sequences, while having excellent spatial resolution, do have lower contrast resolution than other sequences resulting in good anatomic detail but decreased accentuation of lesions. Proton density and T1-weighted images provide good spatial resolution, but T1-weighted images have better contrast resolution due to low signal intensity of fluid in these sequences. T2-weighted and STIR sequences have lower spatial resolution, but improved contrast resolution and are used to characterize lesions by highlighting fluid in bone and soft tissue. STIR sequences are particularly susceptible to motion artifact and magnet field inhomogeneity. When planning protocols, a combination of sequences is used to maximize speed and tissue contrast. [63] Position is important as low-field studies have thicker slices and a smaller field of view. Once pilot images have confirmed that the area of interest is in the isocenter of the magnet, images are typically acquired

in sagittal, transverse and frontal planes. Sequences with short TE such as T1-weighted and proton density may be susceptible to the 'magic angle' effect which results in increased signal intensity. This artifact occurs when the tendon collagen fibers are aligned at 55 ± 10° to the main magnetic field (B_0) due to increased T2 relaxation time. [64] Therefore it is important to use multiple sequence types when evaluating areas of signal hyperintensity in tendons.

MRI studies show good correlation between low- and high-field techniques, and between MR lesions and histopathology.[1, 5-7] The anatomy of the DDFT within the digit based on MRI has been thoroughly described.[65] There is strong left-to-right limb and medial-to-lateral-lobe symmetry of signal intensity and cross-sectional area. The normal DDFT is seen as a bi-lobed, elliptical structure of homogenous low signal on transverse and sagittal MR images.[41] Tendon damage appears as a focal increase in signal intensity within the normal hypointense tendon lobe, with variable enlargement of the affected lobe. DDFT lesions are best seen on T1- and PD-weighted sequences.[5] However, to verify if a signal increase within the tendon is a true lesion, comparison of T1 images with T2 fast spin echo and fat suppressed, STIR images is essential.[41]

In limited re-check examinations of DDFT tendinopathy, it appears that normal signal intensity in T1-weighted images is not re-established despite other sgns of improvement; therefore, MRI may not be able to detect when a sound horse with previous tendon injury can safely return to work. [1] Intravenous contrast agents such as gadopentetate dimeglumine (Magnevist, Bayer Health Care LLC, USA) are widely used in human patients undergoing MR imaging. Considered an extracellular fluid agent, this product increases signal intensity in T1-weighted sequences. Contrast agents can be injected intravascularly to detect capillary breakdown and enhance tissues with increase extracellular volume. Intra-synovial contrast can be used to detect subtle articular cartilage defects and intra-synovial issues. The use of saline as a positive contrast agent has been reported in the navicular bursa of horses, highlighting the presence or absence of adhesions. [66] Contrast-enhanced MRI has been performed in the distal limbs of horses, and DDFT lesions had significantly increased contrast enhancement. [67] It was also noted that more chronic lesions had significantly less contrast enhancement than acute lesions. This may be useful in recheck examinations and predicting the chronicity of healing lesions.

Computed tomography (CT) has historically been used for evaluation of bone lesions; however, its value in soft-tissue imaging of the equine foot has been described. [68] CT is a cross-sectional imaging modality, which maps x-ray attenuation. [16] Image acquisition is rapid, allowing for a complete scan of the distal limb to be performed in < 1 minute. [16] This is beneficial when performing imaging under general anesthesia to limit overall procedure time. Recently, contrast-enhanced computed tomography (CECT) has been shown to have high sensitivity (93%) in diagnosing lesions of the DDFT. [69] Iodinated contrast materials are used to highlight regions of increased vascular perfusion and permeability, which are present in inflammatory and neoplastic conditions. In horses, systemic contrast administration is expensive due to the large dose required for diagnostic images; however, local arterial perfusion can be performed regionally to examine the distal limb. [16] MRI and CT have been compared for imaging the equine foot, with subtle differences noted in the diagnosis of lesion type and location. [69-71] In one study, low-field MRI was more likely to detect lesions distal to the proximal margin of the navicular bone, compared to CT which was more likely to detect lesions proximal to the navicular bone. [70] In another, CECT failed to identify fibrillation and dorsal border lesions at the level of the navicular bone. [69] This is likely due to the high-density flexor cortex of the navicular bone being closely apposed to the DDFT at this level. Also, vascularization associated with these more linear lesions is limited which limits contrast enhancement. The typical DDFT lesions seen on CECT/CT were abrasions, mineralization and enlargement. [70] In comparison, typical low-field MRI lesions were more commonly core lesions and splits. Furthermore, low-field MRI failed to identify soft tissue mineralization and CT/CECT failed to identify bone edema. [70] Contrast-enhancement allowed improved visualization of insertional lesions when compared to pre-contrast CT. Lesions of the DDFT can occur proximal to the navicular bursa, which may be missed on MRI when the radiofrequency coil is centered over the podotrochlear apparatus. [70] It is recommended to acquire additional sequences with the field of view centered over the pastern to ensure more proximal DDFT lesions are not missed. In a DDF tendinopathy case study, the use of contrast-enhanced CT allowed for improved lesion visualization at the dorsal border, when compared to standard high field MRI and CT. [71] Contrast-enhanced CT may also offer the advantage of assessing physiologic changes associated with injury such as new vessel formation and increased vascular permeability, which would help in determining lesion chronicity and monitor healing. Dynamic contrast-enhanced CT studies can help differentiate between these, with early contrast

enhancement being consistent with increased blood flow and contrast retention with vascular permeability. [71] Compared to histopathology, lesions with peripheral contrast-enhancing patterns are associated with collagenolysis and cell necrosis without evidence of tissue repair.[69] Sites that identified signs of neovascularization via contrast enhancement matched highly vascular areas on histopathology.

In summary, different advanced imaging modalities are available for imaging the foot of horses. MRI has traditionally been the method of choice for diagnosis of DDFT lesions; however, both MRI and CT/CECT have potential limitations and there are variations in lesion location and classification. [70] It is important to understand these differences when recommending advanced imaging techniques and interpreting images from CE, CECT and MRI.

Interventional imaging

Interventional imaging is an expanding subset of diagnostic imaging whereby minimally-invasive therapeutic techniques can be performed using imaging guidance. In human medicine, there are many well-established surgical techniques that utilize the advantages of advanced imaging, which have replaced previously risky, invasive procedures. [72] Ultrasonography is routinely utilized for guiding injection of complex or deep joints and other synovial spaces. Radiography is also commonly used for guiding injections and fluoroscopy allows the placement of metallic implants via small stab incisions. With improvements in advanced imaging, CT and MRI have become more available and are now being used for therapeutic techniques.

Navigational ultrasound imaging, or fusion imaging, combines real-time ultrasonography with previously acquired CT- or MRI- images. Fusion imaging software is available on high-end ultrasound units and requires an additional magnetic device placed on the ultrasound transducer, with a nearby GPS to track location. [73] After registering the ultrasonographic images with the CT or MR images by using a series of anatomical landmarks, the CT- or MRI tracks along in real-time with the ultrasonographic exam. The images from both are displayed simultaneously and can also be superimposed on one another. Ultrasonographic-guided intralesional injections with biologic therapeutics are used commonly in treatment of equine musculoskeletal injuries. However, lesions identified on MRI are not always evident on ultrasonography, which makes

targeted therapy difficult. A recent study has examined the use of fusion imaging for facilitating ultrasonographic-guided injections and interventional surgical techniques in horses. [73] Seventeen horses with lesions in a variety of tendon and ligaments in the distal limb were examined. Procedures were performed either standing or under general anesthesia and included intralesional injection with platelet rich plasma, desmoplasty with a ligament knife or curettage. Fusion allowed for visualization of previously unidentifiable lesions on ultrasonography by superimposition of MR images in 31% of cases and confirmed suspicion of the lesion in another 24%. In other cases (28%), the extent and severity of lesions was underestimated with ultrasonography compared with MRI. It was found that the technique was most helpful for lesions of the proximal suspensory ligament, collateral ligaments of the distal interphalangeal joint and oblique distal sesamoidean ligaments. Furthermore, the imaging allowed for avoidance of important neurovascular structures.

CT has also been use to guide surgical techniques and intralesional injections in horses. The three-dimensional advantage of CT was helpful in guiding the transcortical drilling, flushing and packing of subchondral cystic lesions in horses. [74] Puchalski *et al.* (2005) described 12 cases of distal DDF tendinopathy in which a combination of ultrasonography and CT was used to guide intralesional injection with urinary bladder matrix (Acell®, Maryland, USA). [16] An advantage of interventional CT is the ability to rapidly obtain three-dimensional images and the ability to use regular metallic needles and/or instruments. A disadvantage of CT is that horses must be anesthetized.

MRI needle localization techniques are well established in human medicine. [20, 21, 75, 76] Closed bore systems require computer-assisted programs; while open bore magnets improve the efficiency of techniques. [76] More recently, MRI has been used to guide injection of soft tissue structures within the hoof capsule in horses. [18, 77] The open bore, vertical design of the Hallmarq low-field magnet lends itself well to this technique. Traditional closed bore or horizontal magnets require specialized equipment [75] or complete patient re-positioning between scans. [18] A case report describes the combination of ultrasonography with open, low-field MRI to guide injection of a DDFT core lesion with platelet rich plasma. [18] After an initial scan to localize the lesion, the limb was removed from the magnet and aseptically prepared. Needle placement was

guided initially by transcuneal ultrasonography. The limb was then wrapped and placed back in the magnet, using T2-weighted transverse sequences to assess needle location. This procedure had to be repeated twice before adequate positioning was acquired and the injection could be performed. The injection took 90 minutes to complete in this case. The procedure time was likely lengthened by the difficulties associated with the horizontal magnet design. A vertically aligned open, low-field MRI unit was used to guide injection of the collateral ligaments of the distal interphalangeal joint in a cadaver study, and is also reported in a case series. [77, 78] Limbs were positioned to mimic standing, sedated horses and T1-weighted images used with transverse slices for guidance. While procedure time was not recorded, the limb was not moved between reposition attempts, making this likely to be a more efficient technique.

The advantages of MRI for interventional imaging include superior soft tissue contrast and multiplanar imaging capabilities, plus the lack of radiation exposure to personnel. A disadvantage is the signal void produced by the needle, which can be significantly decreased by using non-ferromagnetic materials such as titanium. Various sequences have been reported for needle guidance with MRI, including T2-weighted, [18] T1-weighted [77] and proton-density sequences. [21] It has been reported that needle artifact is more prominent in T1-weighted FSE and GE images than T2-weighted images. [79] Furthermore, needle size affects the void and orientation in relation to B_o, with a more perpendicular position in relation to B_o producing greater artifact. Depending on the structure being injected, there is little that can be done to change the orientation of needle projection. Needle size is a trade off between strength to penetrate tissue without bending and limiting void artifact and tissue trauma.

Due to the relative inaccessibility of the distal portion of the DDFT, intralesional injections have previously been performed with radiographic,[15] CT-, [16] MRI- [18] or bursoscopic [80] control. The radiographic injection technique presented allowed for accurate injection of the DDFT at its insertion onto the distal phalanx. Lesions limited to the insertion have been described in only 6% of horses with digital DDF tendinopathy.[2] At this location, lesions are typically small core lesions, parasagittal splits or osseous changes. To accurately inject a large core lesion is feasible; however, these are rarely present at the insertional level. Lesions of the DDFT within the digit are typically confined to either the medial or lateral lobe, rarely both lobes. [6] The technique

described by Anderson *et al.* (2010) targeted the DDFT on midline, thus, not where lesions typically occur. Therefore, while the technique has merits as it can be performed standing with relatively inexpensive equipment, the number of cases in which injection of the DDFT insertion is necessary is likely low. Furthermore, a diagnosis of digital DDF tendinopathy can only be accurately made with MRI or CT-imaging. Only in chronic, severe cases of enthesiopathy will there be radiographic changes at the facies flexoria of the distal phalanx[41]. Therefore, horses being diagnosed will these lesions will have to attend a facility where these imaging modalities are available, so treatment using these modalities is not common.

Currently reported CT-, MRI- and bursoscopy-guided techniques to inject the digital DDFT require general anesthesia. In many cases, therapeutic biologics take time to prepare, and thus would need to be prepared in advance. Alternatively, the injection would need to be performed during a separate anesthetic event. General anesthesia carries a risk of injury or death, even in healthy horses.[81] It also involves longer preparation and recovery, more clinical staff and additional cost for the owner. Furthermore, horses with injury to the DDFT may potentially be at risk of causing more severe injury during recovery from general anesthesia, especially if large core or multifocal lesions are present. Open, low-field MRI systems have become more widespread in recent years, with 87 units in use in equine clinics around the world. [19] Comparative studies show good correlation between low- and high- field systems.[82] A major benefit of open, LF-MRI systems is that the exam can be performed in standing, sedated horses, thus obviating the risks of general anesthesia and decreasing time, staff and costs involved. Further more, the open magnet design allows full access for needle placement during the procedure, which minimizes procedure time.

Treatment and Prognosis

Treatment options for DDFT tendinopathy are limited and consist of long periods of stall rest with controlled hand walking, and supportive shoeing. [1] The most commonly reported treatment is 4-6 months of rest and rehabilitation, although > 12 months may be needed before returning to full activity. [83] Unfortunately, the prognosis for horses that have been rested for at least 6 months is poor to guarded, with only 25-52% returning to previous levels of athletic

performance. [1, 4, 9 83] If concurrent navicular bone abnormalities are present, the prognosis in one study was worse, with 95% of horses remaining lame. [1] Horses with concurrent navicular bone and DDFT injury may have a completely different etiology to those with primary DDFT lesions. [84] A reduced prognosis has also been reported when adhesions are present to the collateral sesamoidean ligament or navicular bone. [85]

Recently, lesion type has been shown to affect prognosis of DDFT tendinopathy, with significantly more horses with dorsal border lesions returning to some level of work than those with parasagittal split and core lesions. [4] Lesions of the dorsal border area readily accessible via navicular bursoscopy, which can be used to debride these lesions. A series of 92 cases of DDF tendinopathy treated via navicular bursoscopy reported 63% of horses were sound, with 44% returning to previous levels of athletic performance. [10] A similar result was obtained with conservative management of dorsal border lesions, with 72% of horses returning to some level of work. [4] In that study, core lesions (41%) and parasagittal splits (50%) had significantly decreased prognosis when compared to dorsal border lesions (72%). Therefore, it may be the location of these dorsal border lesions, which is important, compared to the treatment. Lesions at the level of the navicular bone compared to those more proximal or distal have an improved prognosis whereas horses with core lesions are less likely to return to athletic performance. The chronicity of lesions may also affect prognosis. In one study, horses lame for less than 8 weeks had a significantly increased likelihood of returning to previous athletic performance than horses with longer lameness periods. [4]

The correlation between lesion severity and lameness has been controversial in the literature. Some studies have reported that degree of lameness is not a significant indicator of outcome. [86] However, retrospective series that look more specifically at DDFT tendinopathy have proposed that the degree of lameness does reflect injury severity. [1, 9] In one study, [9] horses with a higher grade of lameness at admission were less likely to return to full work and no horses with a lesion over 30mm in length or 10% in maximum cross-sectional area returned to work. [9] A more recent retrospective study examined the length of time that horses were able to remain in work. [83] With a median follow up time of 5 years, 61% were able to return to some use, 52% returned to the previous level of athletic use, with a median duration of return to activity of 18 months and 26%

of horses were sound at follow-up. Lesion severity does seem to influence prognosis, with 71% of mild, 64% of moderate and 52% of severe cases returning to use. [83] These results reflect differences in short- and long- term results, with the more long-term soundness of 26% being similar to previous reports on outcome.

Repeat MRI examination of DDFT lesions has shown differences in healing between various lesions. [56] Dorsal border lesions were found to reduce in size significantly over 6 months of conservative management, whereas parasagittal splits and core lesions had only alterations in signal intensity not size. Differences have also been found between sequences when assessing healing of lesions. Horses with lesion resolution on STIR and T2-weighted sequences have a significantly better outcome. [87] This correlation between improved lameness with resolution of hyperintensity on STIR sequences correlates with histological studies, which have shown that STIR hyperintense lesions contain core necrosis, whereas those with normal signal on STIR sequences contain fibroplasia and fibrocartilaginous metaplasia. [40] It is also known that signal intensity typically does not resolve on T1 and PD sequences, which has also been seen in human athletes with injury to the Achilles tendon. [1] However, lesion length and maximum cross-sectional area have been shown to improve on T1-weighted sequences. [56] This can also be explained by histology as we know tendon lesions heal by fibroplasia which results in signal intensity in T1-weighted sequences. [40] Therefore, it is important to use a combination of sequences to assess tendon lesions to help determine chronicity. Furthermore, repeat imaging may be useful in guiding return to performance and prognosis if appropriate sequence interpretation is made.

In a recent retrospective study, it was shown that rest and rehabilitation are an important component of treatment affecting outcome. Horses that were injected with corticosteroids and hyaluronic acid in addition to a 6-month rehabilitation program returned to use for a significantly longer duration than those injected alone. [83] Another factor which affected outcome was the type of performance, with Western performance horses returning to work for significantly longer than English performance horses. As mentioned, an improved prognosis has been reported for DDFT lesions treated with navicular bursoscopy. [10] In a series of 105 bursae examined with bursoscopy, 7 had sagittal splits, which were associated with minimal synovial change and found proximal to

the navicular bone. Fibrillation of the dorsal DDFT was seen in 11 bursae, also with minimal synovial change. The most common lesions were sagittal tears (n=87), of which the majority were classified as extensive (n=63). In these cases, the tears began proximal to the navicular bone and extended distally, with extruded fibers recoiled in the proximal recess of the bursa. Some contained granulation tissue clumps associated with torn fibers, and some showed discoloration and softening of the dorsal surface of the tendon. The torn tendon strands were occasionally found adhered to other structures. Fibrinous adhesions of the DDFT to the navicular bone and lesions of the navicular bone fibrocartilage were also identified in some cases. It is suggested that disrupted collagen in a synovial environment causes persistent inflammation and lameness and no mechanism for intrinsic removal of disrupted collagen from synovial locations has been reported.[10] Therefore, debridement of these lesions appears logical in an attempt to reduce synovitis and facilitate the development of scar tissue at the site of disruption. While this technique has merit, it is limited to lesions that are located in the dorsal aspect of the DDFT at the level of the navicular bursa. The majority of core lesions, which are the target for intralesional injection typically begin further proximal in the tendon. Therefore, while bursocopic-guided injection of DDFT lesions has been reported it is unlikely that true core lesions could be consistently visualized and most of them begin more proximally in the tendon.

Several alternative strategies have been used in the treatment of distal DDFT lesions. These include injection of intrasynovial corticosteroids +/- hyaluronic acid,[86, 88] extracorporeal shock wave therapy,[89] desmotomy of the accessory ligament of the deep digital flexor tendon [41, 90] and intrabursal or intralesional injection of various biological therapies.[16, 17, 89, 91] Intrabursal corticosteroid injection has been shown to alleviate lameness for at least 3 months in 66% of horses. [86] However, the use of corticosteroids in the presence of tendinopathy is controversial and lameness invariably recurs, possibly with accelerated exacerbation of existing lesions.[41, 92] Tendon rupture after local corticosteroid injection has been reported in human patients. [93] A recent case study reported improvement of 3 chronic, severe cases of DDF tendinopathy following desmototmy of the accessory ligament of the deep digital flexor tendon. [90] Transection of this dense, fibrous structure results in lengthening of the musculotendinous unit which decreases the peak extending moment on the DIP at the end of stance phase. [94] It is also thought to decreased tension and loading on the DDFT.

Intralesional injection of regenerative therapeutics has been recommended for improved healing of tendon and ligament injuries.[95] Tendon healing occurs with the formation of fibrous scar tissue, which has inferior biomechanical properties, leading to a high risk of re-injury.[96] Experimental studies have shown considerable promise in the use of intralesional biologic therapeutics for improving tendon healing.[11, 14, 97, 98] It is logical that larger core lesions would be more easily localized and injected than small core lesions, dorsal abrasions or parasagittal splits.[41] The stage of healing is also likely to affect the benefits of and resistance to intralesional injection. Histopathology has shown that core lesions of <6 months duration are comprised of focal necrosis, whereas more chronic (>6 months) lesions consist predominantly of fibroplasia and fibrocartilaginous metaplasia.[40] Injection into an area of degenerative, necrotic matrix would likely meet little resistance and contain the solution within the lesion. Conversely, injecting into an area of fibrous tissue may disrupt the matrix and force apart tendon fibers, thus causing further damage.[80] Recent reports indicate that imaging techniques with contrast-enhancement may be more reliable at predicting the stage of healing of lesions.[16, 67] As intralesional therapeutics become more commonly used, case selection is likely to be an important consideration. Currently it is recommended to perform intralesional injections after the acute inflammatory stage, but before the presence of substantial fibrosis. [29]

Regenerative therapeutics

As previously discussed, the healing of tendon injuries results in fibrous scar tissue. While this may eventually reach a similar tensile strength as tendon tissue, its altered composition leads to impaired elasticity, which reduces performance of the tendon and leads to a high risk of re-injury. [29] There is a low level of matrix synthesis in mature animals, which may be a consequence of cellular senescence, loss of mechanotransduction or growth factor stimulus. The goal of any treatment is to return the tendon as close to normal biomechanical function as possible by normalizing extracellular matrix proteins, longitudinal organization and collagen fiber arragement. Targeted regenerative therapeutics may allow for these goals to be met, resulting in decreased prevalence of re-injury.

Stem Cells

Introduction

Regenerative medicine is a rapidly growing field that aims to repair or regenerate damaged tissues through the implantation of cells, scaffolds or soluble mediators. There has been much research in the use of stem cells for this purpose. Common features of stem cells include the ability to differentiate along different lineages and the ability to self-renew. There are two major types of stem cells described; embryonic and adult stem cells. The embryonic stem cells are derived from the inner cell mass of an early developing embryo. [99] These cells are either totipotent (give rise to endo-, ecto- and mesoderm layer plus placental tissues) or pluripotent (give rise to endo-, ecto- and mesoderm layer but not extra-embryonic tissue). [100] These have potentially unlimited capacity for self-renewal therefore have been of great interest in therapeutic research. However, the generation of these cells results in the death of a fertilized conceptus, therefore their use has ethical considerations, and they have a higher risk of tumor formation. [99] Induced pluripotent cell, in which *in vitro* manipulations are performed to somatic cells to induce a stem-cell like state, are similar to embryonic stem cells and obviate the need to destroy an embryo. [101]

Adult stem cells are capable of self-renewal and have restricted differentiation potential and are therefore called multipotent. They can be obtained from various tissues, therefore are of interest in clinical applications. Fetal-derived stem cells, technically in the adult stem cell classification, can be modified *in vitro* to induce a pluripotent-like state but are not equivalent to embryonic or induced pluripotent stem cells. [11]

Normal tissue development occurs from an initial collection of cells that undergo differentiation into specific tissues, with cells loosing a degree of 'multi-potency' as they become more and more differentiated. Certain tissues, however, retain a population of cells that are capable of replenishing cells throughout life. For example, the blood cell system has a rich population of hematopoietic stem cells in the bone marrow, which is vital for immunity. [99] Also in the bone marrow is a group of cells that form the fibrous 'stroma'; mesenchymal stomal cells or mesenchymal stem cells (MSCs), believed to provide general repair of injury to any mesenchymal tissues in the body, gaining access via the blood stream. MSCs are an excellent

stem cell source for musculoskeletal regenerative therapies as they can be readily obtained from multiple tissues and are of mesodermal lineage, and therefore able to differentiate into cartilage, tendon and bone. [102] Furthermore, they are immune privileged, possibly due to a lack of major histocompatability complex class II expression, which allows for the use of allogeneic cells. They also have immune-modulatory and anti-inflammatory properties and appear to respond to the microenvironment around them. [102] Therefore, the therapeutic potential of MSCs arises from their ability to promote tissue regeneration and inhibit fibrosis through the recruitment of native cells via growth factors and chemotactic signals, anti-inflammation, anti-apoptosis, production of extracellular matrix and stimulation of angiogenesis. [103] These additional effects are known as trophic effects, and are distinct from the direct differentation of MSCs into repair tissue. [104]

MSCs can be isolated from virtually any tissue in the body, and in horses they have been isolated from tendon, muscle, umbilical cord blood and tissue, gingiva and periodontal ligament, amniotic fluid, blood, bone marrow and adipose tissue. [102] The concentration in tissues varies, but overall is low, so *in vitro* isolation and expansion over 2-3 weeks is performed to create cultured MSCs; a relatively homogenous population of cells. The defining criteria for MSCs are 1) adherence to plastic under standard culture conditions, 2) differentiation potential towards osteogenic, chondrogenic and adipogenic lineages, and 3) expressing cluster of differentiation (CD) 29, CD44 and CD 90 and lack of expression of CD34, CD79 and MHC II. [105]

Cell survival and migration after implantation has been studied *in vivo*. A comparison of labeled equine embryonic stem cells (ESCs) and BM-MSCs implanted into SDFT lesions found that cells were present in and around the lesion. [106] However, there were <5% BM-MSC cells still detectable in the lesion 10 days later, whereas ESC survival was high and numbers were maintained over 90 days. A recent study evaluated the location of stem cells labeled with superparamagnetic iron oxide nanoparticles following intralesional injection using MRI. [107] SDF tendon lesions were created surgically with a burr and then injected with labeled BM-MSCs immediately post-euthanasia 10 days later. Post-injection imaging revealed heterogenous and inconsistent cell localization within tendon lesions, with leakage of cells into surrounding tissues in all subjects. The same labeling technique was used to perform long term evaluation of MSC localization in naturally occuring tendon injury in horses. [108] Superparamagnetic iron oxide

labeled allogenic umbilical cord-derived MSCs were injected into SDFT lesions and evaluted with MRI up to 8 weeks post-injection. Following blinded review, MSCs could be distinguished in 6 of 7 SDFTs at 2 weeks and in 4 of 7 SDFTs at 8 weeks. Another study utilized MSCs labeled with technetium-99m hexamethylpropyleneamine oxime to investigate the distribution of cells via intra-lesional administration, regional limb perfusion and intravenously. [109] Following intra-lesional injection, cells were retained in the damaged area, however, by 24 hours only 24% of cells remained in the tendon. The MSCs injected intravenously did not reach the tendon and were mostly distributed to the lungs. Following regional perfusion, there was significant labeling of tendons in 11/12 cases, but not to the same degree as intra-lesional injection. These results are somewhat contradictory to the prior assumption that the majority of a cell bolus is retained within a core lesion. However, these studies do suggest that stem cell "homing" is not effective for localization to tendon lesions, and that injecting cells into the lesion results in the highest concentration at the site of injury, albeit only for relatively short periods.

It has become apparent that the primary role of implanted MSCs in tendon injury occurs indirectly through their effects on tissue regeneration. This included trophic anabolic effects through paracrine and autocrine activity, direct anti-inflammatory effects of the cells, chemoattraction of additional stem cells and anti-apoptotic effects. [103, 104] It appears that these effects decrease ongoing degradation associated with ruptured tendon fibers and the more insidious degeneration associated with ageing and exercise. [97, 104, 110, 111] In equine studies of BM-MSCs and AD-MSCs, the most consistent finding of injected cells has been their anti-inflammatory effects resulting in decreased tendon fiber degeneration compared to controls. [12, 97, 111]

Bone marrow-derived MSCs

Bone marrow is the most commonly used source of MSCs in horses. Studies have estimated that only 0.001-0.01% of mononuclear cells obtained from bone marrow aspirate are MSCs. [112] Furthermore, an age-related decline in bone-marrow MSCs (BM-MSCs) has been found in humans. [113] In contrast, work in horses has shown no difference in MSC numbers collected from bone marrow of foals and young horses. [114] This difference may be due to inadequate numbers, or the use of young horses. There is currently limited data available regarding the number of

cells required for repair of musculoskeletal injuries. Clinical studies have suggested the use of 1 x 10^7 BM-MSCs in naturally occurring SDFT injuries. [12] Harvest sites include the ileum and sternum. There are conflicting reports on which site results in higher BM-MSC yields, with one clinical study showing a significant higher yield from the sternum *versus* tuber coxae. [115] In contrast, another study found that maximum potential yields were 2.1 times greater for ileal than sternal cultures. [116] Volume of bone marrow aspirate has also been evaluated and when collected from the sternum there was significantly higher nucleated cell density in the first 10ml. [116] In the ileum, a higher nucleated cell density was found in the first 5 ml, suggesting that blood contamination occurred after that volume. Interestingly, bone marrow aspirate from the ileum had higher chondrogenic potential than samples from the sternum. Pneumopericardium has been reported as a complication of sternum collection. [117] Recommendations have since been made to collect from the 5th sternebrae as this has adequate dorsoventral thickness and is cranial to the heart. [118] More recently it was found that multiple needle advancements during collection resulted in a initial higher yield of BM-MSCs, compared with a single collection site from the sternum. [119] However, after multiple passages, there were no longer significant differences. The authors suggested that this technique may be more useful when collecting for bone marrow aspirate concentrate, where culture expansion is not performed. A multi-directional needle has also been tested which allows bone marrow collection from three sites without moving the needle. [120] The needle increased the frequency of obtaining 'MSC-richer' BMAC; however, there were no significant increases in MSC concentration.

MSCs have been used in a large number of *in vitro* and *in vivo* laboratory animal studies and have shown improved outcomes over controls. [121-124] In tendon and ligament research, a bioscaffold of collagen gels or sponges, PRP or fibrin is often used in combination with MSCs to fill or support defects. [123, 124] While these animal models provide useful information regarding the potential healing benefits of MSCs, the acute, experimental models of tendinopathy frequently used are quite different from the more chronic tendinopathy typical in horses. Several experimental *in vivo* and clinical studies have investigated the use of BM-MSCs in horses. [12, 14, 111, 125, 126] Experimental studies have investigated how stem cells may improve tendon healing, utilising ultrasonographic examinations, mechanical testing, gene expression, biochemical analysis and histology. Mixed results have been found for ultrasonographic characteristics, with

most *in vivo* studies reporting no significant difference between treatment and control groups in cross-sectional area and echogenicity. [12, 111] In contrast, clinical studies have suggested relatively fast improvements in echogenicity and fiber orientation in treated limbs. [125] Mechanical testing has shown that tendons treated with stem cells have lower stiffness than control tendons, which confers improved functional outcome due to improved elasticity. [12, 111] While no differences have been consistently found in gene expression and biochemical analysis, histology typically shows significant differences between treated and control limbs. Tendons treated with MSCs have improved collagen type I, decreased cellularity, improved crimp scoring and decreased vascularity. [12, 111] A controlled study using naturally occurring SDF tendinopathy showed a significant reduction in water and glycosaminoglycan content of treated tendons and a lower remodeling rate as seen by MMP-13 activity. [12] Sulphated GAG levels are elevated in pathologic tendons so this reduction was considered a positive outcome representative of the normalization of the healing tendon. [12] This study is significant as naturally occurring disease with preceding age-related degenerative changes is much more realistic than experimental acute collagenase or surgical models. Collagen fibril size has also been investigated with no significant difference found between control and MSC-treated tendons. [126] While the exact mechanism by which MSCs improve tendon healing is not known, there has been increasing evidence in clinical studies of MSC efficacy. One of the larger clinical series (n=141 horses) investigated the intralesional injection of MSCs in naturally occurring SDF tendinopathy and compared results to historical controls. [14] For National Hunt horses there was a significant reduction in re-injury rate (25.7%) compared to other treatment methods. This difference was not found for flat racing horses, although this group was smaller so horse numbers may not have reached statistical significance. No differences were found between the timing of injection, number of MSCs injected or age of the horse. Other smaller clinical studies show similar results, with decreased re-injury rate, suggested improved quality of repair, being the most commonly reported benefit of MSC treatment. [125]

Adipose tissue-derived MSCs

Adipose tissue has been used in limited clinical trials as a source for cultured stem cells. The proliferative potential and yield of adipose-derived stem cells is reportedly higher than that of BM-MSCs. [127, 128] They are capable of multi-lineage differentation, although evidence indicates

that they may be less capable of generating osseous or cartilaginous tissues than BM-MSCs but are particularly potent as immunomodulatory agents. [129] One found that adipose-derived MSCs expressed significantly higher levels of tendon specific extracellular matrix proteins than MSCs from other sources, suggesting that these cells may be superior with regard to positive influence on tendon matrix reorganization. [130] Another study showed wdipose-derived stem cells were less effective at forming tendon than either bone marrow- or tendon-derived stem cells. Adipose tissue can be harvested from pericoccygeal, sternal or inguinal fat deposits, with pericoccygeal being most common due to easy access, minimal vascularity and high yield. [131, 132] More commonly in clinical practice, adipose tissue is used to make vascular stromal fraction, which has a fast turn-around time and is less expensive than culture expanded MSCs. When using adipose tissue for vascular stromal fraction it is recommended to collect 15-20g of adipose tissue for processing. [97] In contrast, a smaller amount of only 3-4g of adipose tissue has been found sufficient when cells are cultured expanded to make AD-MSCs. [133] MSCs can be isolated from solid tissues such as adpiose via digestion using proteolytic enzymes like collagenase. [134]Alternativley, an explant technique can be used, whereby tissue is cut into small sections and plated onto plastic culture, after which MSCs migrate and adhere to the plastic culture. Studies have investigated the advantages and disadvantages of these techniques, with some variation between papers. Enzymatic digestion appears to generate a higher initial yield of MSCs, with no major differences between techniques in cell characteristics. [134]

The localization of AD-MSCs has been evaluted in horses via multiple techniques. One study labeled AD-MSCs with a fluorescent antigen and superparamagnetic iron oxide (SPIO) particles and then injected them into experimentally induced SDF tendonitis lesions. [135] Tracking was performed via low-field MRI examination *in vivo*, and then via histopathology following euthanasia at various time points up to 9 weeks post-injection. Fluoresence tracking of labeled cells showed AD-MSCs at and near the injection site in all horses up to 9 weeks post-injection, with a subjective decrease in number of cells over time. Hypointense signal voids correlating with SPIO particles were seen on MRI examinations at the injection site up to 62 days post-injection. Another study used nanocrystal labeled AD-MSCs injected into collagenase induced SDFT lesions. Peripheral blood samples were collected post-injection and SDFT biopsies from treated and control limbs were analyzed 1 week after injection. Labeled AD-MSCs were found in

peripheral blood and the SDFT lesions up to 7 days post-injection. There were no labeled cells present in the contralateral, control limb. [136]

AD-MSCs have been used less frequently in clinical and experimental studies, but have shown positive results in horses. An experimental equine study found increased neovascularization in SDF tendons after intralesional injection of AD-MSCs, as evidenced by Doppler ultrasonography, histopathology and immunohistochemistry. [137] A similar experimental model was used in another study and then SDFT lesions injected with AD-MSCs. [138] Although no differences were seen in clinical or ultrasonographic analysis, there was significant improvements in tendon fiber organization on histopathology and increased collagen type I on immunohistochemistry. Allogeneic AD-MSCs have been used in combination with PRP in two clinical case series of SDF tendonitis, with no reported adverse reactions. [139, 140] AD-MSCs have been used in combination with PRP in a small clinical study of naturally occurring SDF injuries, with no complications and subjectively improved re-injury rate. [13]

Fetal-derived and embryonic-like stem cells

As mentioned, early-stage fetal tissue has been used to develop an embryonic-like stem cell line that has the markers of ESCs but without the teratogenic potential, and have the potential for allogenic use. Evaluation of these cells in an equine experimetal study showed significant advantages. Intralesional implantation resulted in improved ultrasonographic density within 4 weeks, and tissue harvested at 8 weeks showed significant improvements in MRI, histologic and gene expression profiles indicating improved healing. [11] Furthermore, another study found that ECSs had significantly improved survival time than MSCs when injected into tendon lesions. [141] *In vitro* work has suggested that ESCs, like MSCs, express MHC I but not MHC II. [142] In culture, equine ESCs did not affect baseline allogenic peripheral blood mononuclear cell proliferation, even after differentiation and exposure to IFN-γ. Induced pluripotent stem cells (iPS) are another line of stem cells that can be developed as an allogenic cell for immediate use. [143] They also have the benefit of not requiring collection of embyronic or fetal tissues which alievates ethical concerns. These cells are created by genetically re-programing adult stem cells, via various methods such as using viral vectors. The development of iPS from adult fibroblasts has been reported in horses, with these cells displaying properties of pluripotency. Futher work

by the same research group showed that iPS could be induced to differentiate into MSC-like populations. [143] These cells could potentially provide a new source of MSCs with enhanced proliferation and differentation capabilities. The immunogenicity of equine iPS has been investigated by intradermal injection in horses. [144] The cells weakly expressed MHC molecules and elicited no systemic response, however, there was mild inflammatory reaction at the injection site.

MSC concentrates

It has been suggested that the ideal time to implant stem cells is after the inflammatory phase and before the fibrous tissue phase. A clinical study showed that delayed BM-MSC implantation (83 vs. 44 days) negatively affected outcome. [35] As cultured MSC techniques typically take 2-3 weeks for adequate cell expansion, this can cause a delay in treatment of lesions. For more expedient treatment options, patient-side kits are available for faster turn around of samples from bone marrow and fat. [102] These options allow for earlier treatment of lesions and are significantly less expensive than cultured MSCs. For bone marrow, this preparation is referred to as bone marrow aspirate concentrate (BMAC) and contains white blood cells, platelets, hematopoietic stem cells and growth factors in addition to the small numbers of MSCs. The increase in MSC concentration of the mononuclear fraction of BMAC compared to unprocessed bone marrow is well accepted and reported across many species. In horses, there is a 5- to 19- fold increased in MSC concentration after processing, also with increases in white blood cells and platelets and decreases in red blood cells. [120] Point-of-care systems produce BMAC via either density gradient or centrifugation systems, with the advantage of it being a 1-step nonlaboratory process. The final preparation contains the nucleated cell fraction as well as plasma; an excellent source of growth factors. In human medicine, BMAC has been used in orthopedic procedures such as cervical vertebral fusion and nonunions, therefore there may be application for the use of BMAC in equine fracture repair. [129] BMAC has been tested and compared to cultured BM-MSCs in an experimental equine study. [98] Both preparations equally benefited tendon repair, with significant improvements in collagen I/III ratio and COMP expression compared to controls.

Adipose-derived stromal vascular fraction cells (ADSVFCs) or adipose –derived nucleated cell (ADNC) fraction can be produced from adipose tissue. A relatively simple technique of digestion, separation and concentration is used to create a heterogenous population of cells including MSCs, endothelial progenitor cells, hematopoietic stem cells and fibroblasts. With a fast turn-around time of 24-48 hours, these cells can be used for immedate use or can be culture expanded for additional treatments. ADNC fraction has also been evaluated in an experimental equine study. From 20g of adipose tissue, ADNCs ranged from 1.47-2.71 x 10^6 cells/g with a viability of 83-91%. [97] Treated tendons had improved histologic scores for tendon architecture and decreased vascularity, inflammatory cell infiltrate and collagen type III. [97] There were improvements in tendon fiber density and alignment, and increased levels of COMP on gene expression.

Platelet Rich Plasma

Platelets are produced by megakaryocytes in the bone marrow and circulate in the blood for around 10 days. [145] Platelets are critical in the first phase of healing of any tissue injury, the inflammatory phase. At a site of injury, they become activated and release intracellular stores of multiple growth factors and proteins contained within α-granules. Important growth factors include platelet derived growth factor (PDGF), transforming growth factor (TGF), fibroblast growth factor (FGF), endothelial growth factor, hepatocyte growth factor and vascular endothelial growth factor (VEGF). [145] VEGF is a powerful angiogenesis stimulator. TGF influences cell migration, proliferation and replication. PDGF has a chemotactic effect on monocytes, neutrophils, fibroblasts, mesenchymal stem cells and osteoblasts. FGF is an important mitogenic factor for fibroblasts and endothelial cells. Therefore, through the secretion of chemokines, platelets modulate inflammation and attract leukocytes and monocytes to the injured tissue. In tendon healing, fibroblasts are crucial and contribute to the resolution of inflammation. Platelets are also major source of platelet factor-4 which activates fibroblast migration. Platelets also support angiogenesis through growth factors targeted at increasing vessel wall permeability and recruiting the growth of vascular cells (notably VEGF).

Platelet Rich Plasma (PRP) is one of many terms used in the literature to describe concentrated platelet preparations. [146]With the variety of commercial PRP kits available, there are many

differences in the final preparation, including platelet numbers, growth factor profiles and concentration, white cell numbers and inflammatory cytokine profile. Reports of failures in clinical cases may be due to this wide variation in available preparations. A classification scheme for PRP has been suggested, based on by the presence or absence of leukocytes, the manner in which platelet activation occurs and the absolute number of platelets. [146] There are two ways to make PRP; plasma-based and buffy-coat based. [146] Plasma-based methods aim to isolate only plasma and platelets and remove white blood cells. Some platelets are left behind with the intent to exclude leukocytes, thus a slow, short spin cycle is used during centrifugation. Typically 2x - 3x platelets compared to blood baseline are yielded. Buffy-coat methods isolate a platelet-poor plasma and buffy-coat layer, which also contains leukocytes and red cells. During the centrifugation process, high spin rates and long spin regimes are used to capture all available platelets and also obtain a high concentration of white cells. Between 3x-8x baseline platelet concentrations are typically yielded with this technique. The differences between commercial PRP preparations are important to consider when analyzing and comparing outcomes of clinical studies, however, this information is not always reported. The optimum concentration of whiter blood cells in PRP has been investigated. In an equine tendon explant model, there was increased expression of proinflammatory cytoines IL-1β and TNF-α in the leukocyte-rich PRP group. [147] This was also demonstrated using human PRP, with the leukocyte-rich group having significantly increased catabolic enzymes. [148] The same research group has compared three PRP preparations with the same platelet count but varying white cell numbers and found no difference between anabolic cytokines between groups, but increased catabolic cytokines in the leukocyte-rich preparation. [147] They also investigated platelet to white cell ratio, but found no protective effect of increased platelets on reducing catabolic cytokines. Interestingly, a 'biologic threshold' for platelet numbers was found whereby further increases in platelet numbers did not result in greater anabolic upregulation. [149]

Studies have shown that a single intratendinous injection of PRP increases neovascularization compared to placebo-injected controls for at least 23 weeks. [150] *In vitro* studies using equine tendon explants have shown increased expression of collagen genes with no increase in catabolic molecules. [151] Similar results were seen in human tendon cell culture. [152] Experimental studies in laboratory animals have more mixed results on the clinical benefits of PRP. In a rabbit patellar

tendon injury study, there was a significant difference between PRP-treated and control groups at day 14, but by 28 days post-injection there were no differences in histological or biomechanical properties. [153] In contrast, a rat Achilles tendon transection model showed improved material characteristics in the treatment group. [154] PRP has been used fairly extensively in human sports medicine for tendinopathy and other injuries. A clinical study used PRP to treat chronic tendinopathies in the Achilles tendon, but found no significant differences in the treatment *versus* control groups. [155] However, an improvement was seen in level of pain after a single PRP treatment in patients with chronic elbow tendinosis in another study. [156] In a double-blind, randomized controlled study in humans with chronic lateral epicondylitis, a significant difference was seen in the PRP group compared to the corticosteroid group 1 year after treatment. [157] The lack of consistency between these reports is likely due to differences in PRP preparations and individual variation.

Experimental and clinical studies have investigated the use of PRP in horses with tendon and ligament injury. [13, 150, 158, 159] In an experimental, *in vivo*, placebo-controlled study in horses, significant improvements were seen in tendon healing following intralesional injection of PRP. [158] This included an increased strength at failure and elastic modulus. There was also increased cellularity, glycosaminoglycan and collagen content and improved histology scores. While improved histology scores are indicative of improved healing, increased cellularity and GAG content has previously been considered a change that occurs with pathology. [12, 160] Another experimental, controlled study found improved organization on histology 36 days after intralesional injection of PRP. [159] A possible synergistic effect has been suggested between MSCs and PRP, which are often used in combination in clinical cases. An experimental study in sheep investigated this, and did find significant differences between treatment groups. [161] However, the differences between groups suggested a major influence of the MSCs, with no additional benefit of PRP. Equine clinical studies also report the combined used of MSCs with PRP; however, it is difficult to determine if the positive effects seen are the result of MSCs or the PRP. [139, 162]

Autologous conditioned plasma (ACP) is a leukocyte-reduced platelet concentrate that falls under the broad category of PRP preparations. The goal is to concentrate platelets and growth

factors while decreasing white cell numbers to reduce the concentration of catabolic enzymes. This preparation has been used in an experimental, controlled equine study using surgically induced lesions of the superficial digital flexor tendon. [163] There were no significant differences found in ultrasonographic, biochemical, biomechanical and histological parameters between treated and control limbs except for a significant decrease in sulphated glycosaminoglycans. The ACP had similar platelet numbers to whole blood and decreased white cell numbers, with increased levels of PDGF. When compared to PRP studies using similar equine models, it seems that PRP may have more of a profound effect on tendon healing than ACP. [150, 158, 164]

Conclusions

From the literature, it is clear that the use of biological therapeutics for tendinopathy is increasing, with growing experimental and clinical evidence of the healing benefits. As the distal portion of the DDFT is more difficult to image for interventional treatment with traditional methods such as ultrasonography, an imaging guidance technique is necessary to inject the tendon at this location. With the increase in availability of open, low-field MRI units across the world and the fact that MRI is used to diagnose these lesions, utilizing this imaging modality for injection guidance would be ideal. Furthermore, the ability to perform the technique in standing horses would reduce risk and increase utility of the technique. While further work is needed to determine the optimal time frame for injection, the most useful biologic preparation and the efficacy for DDF tendinopathy, intralesional injections are currently being performed routinely in tendinopathy cases. Therefore, a technique by which an accurate injection of the distal DDFT could be performed in standing horses would be clinically relevant and useful.

CHAPTER 2

Accuracy of Open MRI for Guiding Injection of the Equine Deep Digital Flexor Tendon within the Hoof.

Lauren M. Groom, Nathaniel A. White II, M. Norris Adams, Jennifer G. Barrett

Abstract

Lesions of the distal deep digital flexor tendon are frequently diagnosed using magnetic resonance imaging in horses with foot pain. Intralesional injection of biologic therapeutics shows promise in tendon healing; however, accurate injection of DDFT lesions within the hoof is difficult and requires general anesthesia. The aim of this experimental study was to evaluate accuracy of a technique for injection of the deep digital flexor tendon within the hoof using MRI-guidance, which could be performed in standing patients. We hypothesized that injection of the DDFT within the hoof could be accurately guided using open low-field MRI to target either the lateral or medial lobe at a specific location. Ten cadaver limbs were positioned in an open, low-field MRI unit to mimic a standing horse. Each DDFT lobe was assigned to have a proximal (adjacent to the proximal aspect of the navicular bursa) or distal (adjacent to the navicular bone) injection. A titanium needle was inserted into each tendon lobe, guided by T1-weighted transverse images acquired simultaneously during injection. Oil-based colored dye was injected as a marker. Post-injection MRI and gross sections were assessed by three blinded investigators experienced in equine MRI. The success of injection as evaluated on gross section was 85% (70% proximal, 100% distal). The success of injection as evaluated by MRI was 65% (60% proximal, 70% distal). There was no significant difference between the success of injecting the medial *versus* lateral lobe. The major limitation of this study was the use of cadaver limbs with normal tendons. The authors conclude that injection of the DDFT within the hoof is possible using MRI guidance.

Introduction

The foot is a common source of pain in horses and the deep digital flexor tendon is the most commonly injured soft-tissue structure within the foot. [1] Injury of the deep digital flexor tendon within the hoof is predominantly a magnetic resonance imaging diagnosis and MRI studies have identified injury of the deep digital flexor tendon within the hoof as the primary cause of lameness in 10-43% of cases. [1-4] Studies show good correlation between low- and high-field MRI, and between lesion appearance and histopathology. [1, 5-7] Deep digital flexor tendon lesions are classified into 4 categories according to location and appearance on MRI: core lesions, parasagittal splits, dorsal abrasions and insertional lesions. [2] Lesions of the deep digital flexor tendon occur most commonly at the level of the navicular bone and proximal aspect of the navicular bursa. [8] The distribution of lesion type varies with location, with core lesions predominating at the level of the proximal interphalangeal joint. [8] At the level of the navicular bone and proximal aspect of the navicular bursa, dorsal abrasions are most common, followed by core lesions and parasagittal splits. Lesions are typically confined to either the medial or lateral lobe. [2]

Treatment options for deep digital flexor tendinopathy are limited, consisting of long periods of stall rest with controlled hand walking and supportive shoeing. [1] The prognosis is poor, with only 25-28% of patients returning to previous levels of athletic performance. [1, 4, 9] Navicular bursoscopy is recommended to debride dorsal, intrabursal lesions, with 42% of patients returning to previous level of athletic performance. [10] Several alternative strategies have been used in the treatment of digital deep digital flexor tendon lesions, including intrabursal or intralesional injection of various biological preparations. [11-13] Experimental studies and limited clinical trials have shown considerable promise in the use of intralesional biologic therapeutics for improving tendon healing. [11-14] Ultrasonographic-guidance is used routinely in clinical cases to inject tendon lesions in the pastern and metacarpal/metatarsal regions.

Due to the relative inaccessibility of the distal portion of the deep digital flexor tendon, intralesional injections have previously been performed with radiographic, [15] CT- [16] or bursoscopic [17] guidance. The radiographic injection technique allows for accurate injection of the deep digital flexor tendon on midline, at its insertion onto the distal phalanx. Lesions limited to

the insertion only occur in 6% of horses with digital deep digital flexor tendinopathy [2] and lesions typically occur in the medial or lateral lobe. [6] Therefore, while the technique has merit, it has limited utility due to the small percentage of cases with this specific lesion. Both CT- and bursoscopic-guided techniques to inject the distal deep digital flexor tendon require general anesthesia. Low-field, open magnet MRI (Hallmarq Veterinary Imaging, Guildford, Surrey, UK) systems are becoming more available, with 87 units in use in equine clinics around the world. [19] A major benefit of open magnet MRI systems is that the exam can be performed with the horse standing. Core lesions at the level of or just proximal to the navicular bone are the predominate target for intralesional injection. MRI offers several key advantages, which make this difficult technique more accurate. This includes the ability to rapidly obtain multiple thin slices in various orthogonal planes and excellent anatomical soft tissue detail; all without radiation exposure to personnel. MR imaging has been used extensively in human medicine to guide injection of various soft tissue structures. [20, 21] Closed bore systems require computer-assisted programs; while open bore magnets improve the efficiency of techniques. [76]

A standing, open MRI-guided injection technique of the deep digital flexor tendon has been used in 4 clinical cases in our hospital (Figure 1). Further investigation of this technique is warranted, as there are currently no validated methods available for injecting the distal portion of the deep digital flexor tendon in standing horses. The aim of this study was to evaluate the accuracy of a technique for injection of the deep digital flexor tendon within the hoof using MRI-guidance, specifically targeting either the medial or lateral lobe, at a pre-determined site. We hypothesized that injection of the deep digital flexor tendon within the hoof could be accurately guided using low field open MRI to target either the lateral or medial lobe at a specified proximal or distal location.

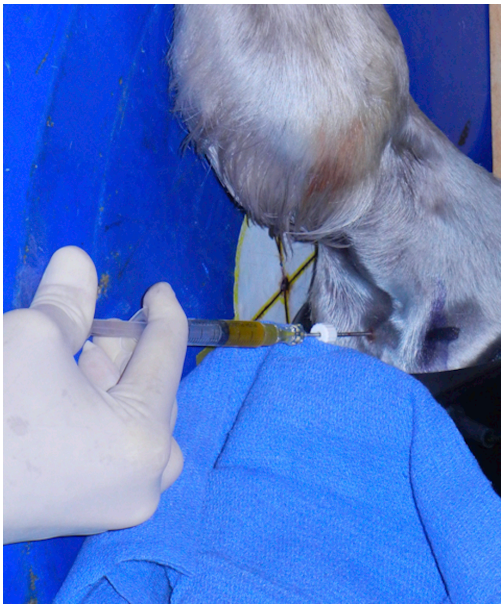

Figure 1- A clinical case of deep digital flexor tendinopathy being injected with bone marrow-derived MSCs using open, low-field MRI guidance.

Materials and Methods

Experimental Design

In this experimental study, equine cadaver limbs were collected and prepared to mimic a standing horse presented for DDFT injection.

Specimens

Ten cadaver forelimbs were collected from 5 horses with no history of forelimb lameness and euthanized for reasons other than this study. Limbs were selected for inclusion in the study by LMG. Bilateral front limbs were amputated through the mid radius, proximal to the origin of the accessory ligament of the superficial digital flexor tendon. Limbs were labeled and frozen at -20°C until needed. All limbs were harvested and frozen within 6 hours of euthanasia. After thawing for 24 hours at 4°C, hair was clipped circumferentially from the fetlock distally. A 4.5mm hole was drilled through the dorsal cortex of the proximal radius and through the hoof capsule at the toe. A double loop of 50# monofilament nylon was placed through these holes and tension applied subjectively to align the third metacarpal bone vertically to mimic limb position of a standing horse. A standard dorsal 60° proximal-palmarodistal radiograph (Sound Vet Sprint Air Ultralight digital radiography system with Minray TR90 portable x-ray generator) using a

kVp of 76 and mAs of 1.0 was taken of each hoof and any metallic fragments removed prior to MR imaging.

Pre-injection MRI

The limb was centered on a 20°C angled wedge block, in a dedicated hoof radiofrequency coil. This arrangement simulates the position of a standing sedated horse's thoracic limb during MRI-guided deep digital flexor tendon injection in clinical patients (Figure 2). Standard, three-plane pilot images were acquired to ensure placement of the digit in the isocenter of the magnet and to facilitate sequence planning. Baseline transverse and sagittal MRI studies were performed using T1-weighted, three-dimensional, gradient echo (T1W GE) and short tau inversion recovery, fast spin echo (STIR FSE) sequences with an open 0.27 T magnet and extremity radiofrequency coil (Hallmarq Veterinary Imaging, Guildford, Surrey, UK). Images were assessed (LMG) and any specimens with pathology of the deep digital flexor tendon were discarded. The following pulse sequence parameters were used throughout the study: repetition time (TR) 23ms, echo time (TE) 7 ms, flip angle 40◦, number of acquisitions (NEX) 1, slice thickness 5.0 mm, field of view 16.9 cm, matrix size 256 Å~ 256, acquisition time 126 s.

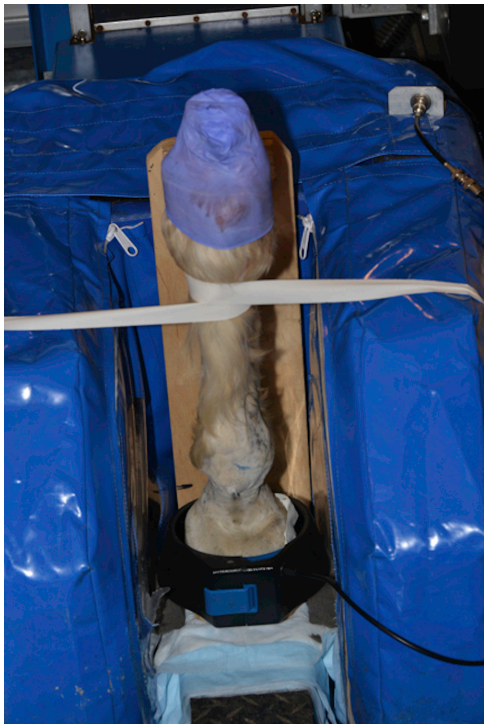

Figure 2- Cadaver specimen prepared and positioned to mimic the configuration of a standing, sedated horse.

MRI-guided injection

The investigator (LMG) performing the injections had no prior experience with MRI-guided and minimal experience with radiographic- or ultrasonographic-guided injection techniques. A 16-gauge x 10cm, nonferromagnetic titanium needle (Invivo Puncture needle, Ivivo, Gainesville, FL, USA) was used for the technique. Injections were performed in either the medial or lateral lobe of the deep digital flexor tendon, targeting either the proximal or distal location as defined by: adjacent to the proximal aspect of the navicular bursa (proximal) and adjacent to the navicular bone (distal).

The medial or lateral lobe was assigned to the proximal location by random number generation, and then the other lobe was used for the distal location. The injection location was determined by palpating the abaxial margins of the deep digital flexor tendon in the distal palmar pastern. The needle was inserted through skin, half a centimeter off midline (medial or lateral), just distal to the proximal edge of the ungulate cartilage in a distal-dorsal direction. A real-time imaging

technique, which consisted of overlapping series of two transverse, T1W GE images, was taken as the needle was advanced. This allowed the needle to be visualized as it was inserted into the tendon (Figure 3A, 3B). Each time the needle was advanced, two more slices were taken to identify the needle tip. It was easy to identify the needle void on transverse MR images, and when it was seen to travel towards the wrong lobe (too far axial), the needle was re-positioned. If there was question regarding the angle of insertion, 4 Tl-weighted sagittal plane images were taken through the target lobe. A steeper angle was used for the distal location, but the needle entry point was the same for both locations. Once the needle was in the desired location, or after a maximum of 4 re-positioning attempts, the stylet was removed and 3ml colored oil-based dye (blue or orange AmeriColor Oil Candy Color, USA) mixed with mineral oil was injected using a 3ml luer-lock syringe. Resistance to injection was subjectively graded as minimal, moderate or marked and time from beginning the technique to removing the needle was recorded. Before removing the needle, a ruler was used to measure the needle from skin to hub and this was subtracted from overall length to give needle depth.

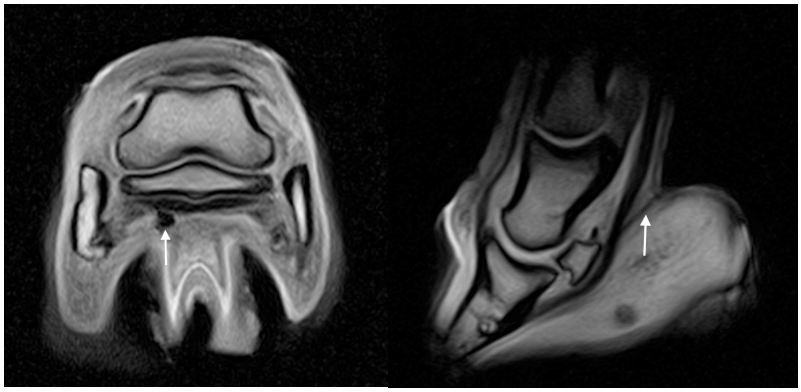

Figure 3: A (left): Transverse T1-weighted MRI slice showing the signal void due to needle artifact (arrow) approaching lateral lobe of DDFT. B (right): Sagittal T1-weighted MRI slice showing needle artifact (arrow) in DDFT at the proximal location.

Post-injection analysis

T1 GE transverse and sagittal MR images were obtained from all limbs immediately after injection. The limbs were then frozen at -20°C for a minimum of 24 hours to set the dye solution. A band saw was used to section the limbs in the transverse plane, at 1cm intervals to match the angle of the MRI slices. The first slice was made at the proximal interphalangeal joint and continued until no further colored dye was present. Sections were labeled and photographed for

further analysis. One representative image was selected from each location (proximal, distal) from each modality (MRI, gross dissection) from each limb. An assistant (EM) created 3 copies of each image, removed identifying information and randomly scrambled the order of images for analysis. Three blinded investigators familiar with equine anatomy and musculoskeletal MRI (NAW, MNA and JGB) reviewed images independently, assessing the presence and location of colored dye or hyperintense oil (injectate). Scores were assigned to each DDFT lobe and key synovial structures; the navicular bursa, digital tendon sheath and coffin joint. A zero score was assigned for no injectate within the structure and a score of 2 for injectate present within the structure. In addition, when assessing tendon lobes, a score of 1 was assigned when injectate was present within and crossing the margins of the structure. Scores were independently recorded in a spreadsheet and the images were then un-blinded for statistical analysis. During this process, if both dyes were seen in the same section, the 'unexpected' color was determined to be a needle tract. A successful injection was defined as injectate within the targeted lobe at the target location. Injections were considered marginal when injectate was present within but crossing the border of the targeted lobe at the target location. Unsuccessful injections contained no injectate within the targeted tendon lobe at the target location. The presence of injectate in synovial structures was recorded but had no influence on the success of injection.

Data analysis

Data was entered into an Excel spreadsheet for initial analysis and then a commercially available statistical analysis program was used for further evaluation (JMP® Software, Cary, NC, USA). All statistical analysis was performed by LMG and JGB. The mean and median procedure time, needle depth, number of attempts and resistance to injection was determined. The frequency of injection success was calculated to assess accuracy at each injection location. The difference in success between the proximal and distal location was compared for each modality with a Chi-squared test. The difference between success for medial and lateral lobes was compared with a Students T test. The difference in resistance to injection between proximal and distal sites was compared with an unpaired T test. Statistical significance for all tests was set at $p \leq 0.05$.

Results

The 5 horses from which pairs of thoracic cadaver limbs were collected had an average age of 17 years (range 15-18 years), with 4 geldings and 1 mare. There were 2 Thoroughbreds, 2 Quarter Horses and a Draft cross. In total 20 injections were performed; 10 targeting each lobe of the deep digital flexor tendon and 10 targeting each location. The median procedure time, from beginning the injection to removing the needle was 8 minutes (range 6-17 minutes) (Graph 1). The median needle depth was 3.55cm for the proximal location and 4 cm for the distal location. A median of 1 attempt was required for each injection (range 1-3). The resistance to injection was subjectively recorded as marked in 1 proximal and 8 distal injections, moderate in 6 proximal and 0 distal injections and minimal in 3 proximal and 2 distal injections. There was subjectively greater resistance to injection at the distal compared to the proximal location (p=0.03). Synovial structure injection was recorded in all injection attempts (Graph 2). Subjectively, the needle was easy to identify as a hypointense void and could be followed as it progressed closer to the tendon in sequential transverse images.

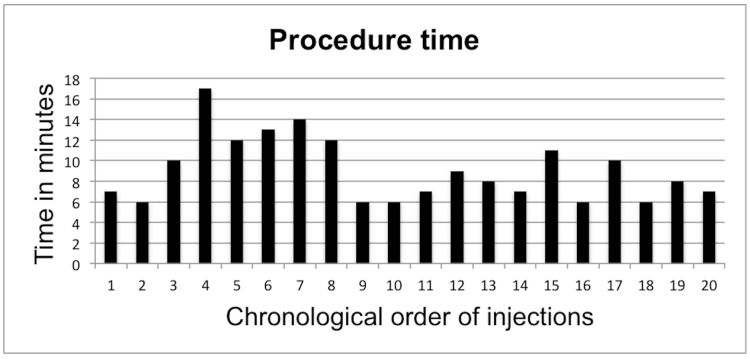

Graph 1: Procedure time for each injection in chronological order. Time was recorded from moment needle penetrated skin to the moment the needle was removed.

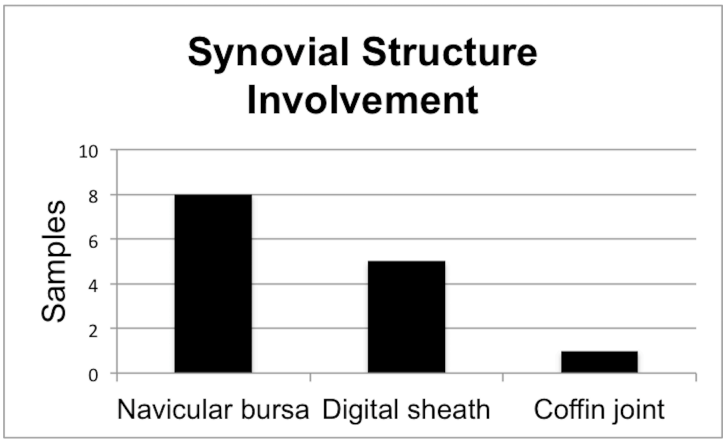

Graph 2: Location of synovial structure involvement in each sample.

The injection success rate as evaluated by gross dissection (Figure 4A
, 4B) was 85%, with 70% of proximal and 100% of distal injections marking the target location. The injection success rate as evaluated by MRI (Figure 5A, 5B) was 65%, with 60% of proximal and 70% of distal injections marking the target location. There was no significant difference between the proximal and distal locations as evaluated by gross dissection (p=0.06) or MRI (p=0.63). When assessing the overall success rate based on both modalities (MRI, gross dissection), there were only 2 specimens that were deemed unsuccessful by both. There were 5 false negative results for MRI and 2 false negative results for gross dissection. As evaluated by gross dissection, the success rate for the lateral lobe was 70% and medial lobe 90%. As evaluated by MRI, the success rate for the lateral lobe was 60% and medial lobe 70%. There was no significant difference in success between the lobes as evaluated by gross dissection ($p=0$.14) or MRI (p=0.33). There was no occasion whereby the incorrect lobe was injected.

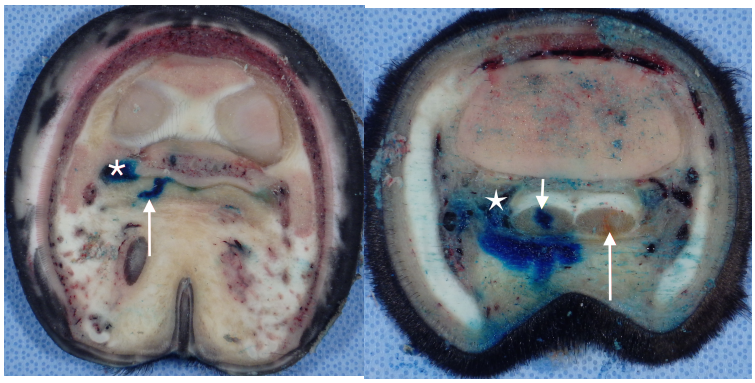

Figure 4. A (left). Gross specimen in transverse section demonstrating a successful distal injection. Blue dye is indicated by the arrow. Note the blue dye staining in the navicular bursa (star). B (right): Gross specimen in transverse section demonstrating a successful proximal injection. Orange dye is indicated by the long arrow. Note the blue dye staining in the digital sheath (star) and needle tract (short arrow) in the other tendon lobe.

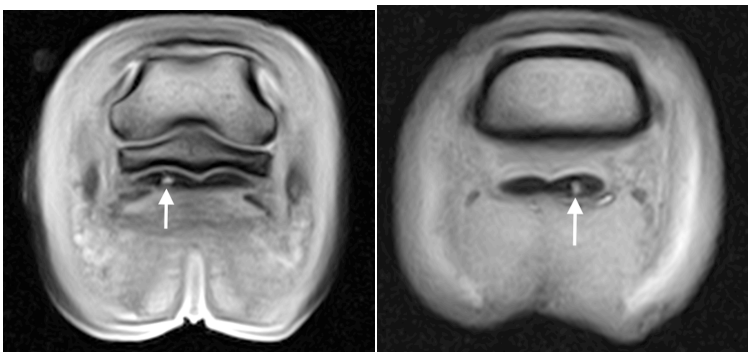

Figure 5. A (left): Transverse, T1-weighted MRI image of a successful distal injection. Hyperintense oil is indicated by the arrow. B (right): Transverse, T1-weighted MRI image of a successful proximal injection. Hyperintense oil is indicated by the arrow.

Discussion

This study describes and evaluates an MRI-guided technique for injecting the deep digital flexor tendon within the hoof in standing horses. The results of this study support our hypothesis that open MRI can accurately guide injection of the deep digital flexor tendon within the hoof, targeting either the lateral or medial lobe at a specific proximal to distal location. The technique is intended to be useful for lesions at any location within the hoof capsule. The navicular bone and proximal aspect of the navicular bursa were chosen to target in this study, as these are the

most commonly reported location for lesions of the deep digital flexor tendon to occur within the hoof. [8] Each target location, proximal and distal, measured 2cm in length. As the center of each lobe was targeted, the target cross sectional area within each lobe was approximately 0.2cm^2. This yields a target area of approximately 0.4cm^3.

The proximal location had a lower success rate than the distal location (70% vs. 100% as evaluated by gross sections), which may be secondary to the limitations of a cadaver study. Ante mortem and post mortem MRI studies on the same horses have shown no significant differences in MR images. [7] Therefore, the use of cadaver limbs should not affect MR image appearance. However, the tendon laxity inherent to cadaver limbs subjectively made needle positioning more difficult at the proximal location. At this level, the tendon is not supported between the firm digital cushion and navicular bone, which allows the tendon to move medial to lateral and dorsal to palmar as the needle is manipulated. This problem has not been noted in clinical cases as weight bearing results in a taut tendon, allowing for more precise needle positioning and fine movement during redirection. This is also a benefit of performing the injection in a standing horse *versus* a recumbent, anesthetized horse. The tension of the deep digital flexor tendon was standardized in this study by isolating limbs proximal to the origin of the accessory ligaments of both the deep digital flexor tendon and superficial digital flexor tendon, and securing the limb in a standard, weight bearing position. However, the tension on the deep digital flexor tendon was unlikely to be equal to a standing horse. There was no significant difference in success between the medial and lateral lobe. Furthermore, there were no occasions whereby the incorrect lobe was injected.

The use of normal, non-diseased tendons may have lowered the success rate compared with what might be possible in live patients, as substantial force was required to force the injectate into the dense structure of a normal tendon. This caused leakage of solution into the needle tract and surrounding tissues, especially if the needle tip was close to the epitenon. Another contributing factor for a lower success rate at the proximal location was the presence of fibrocartilage in the dorsal 30% of the tendon. If the needle was located in this part of the tendon, injection was very difficult and the injectate would leak around the needle. From clinical experience, the authors

have noted that injecting into a core lesion encounters minimal resistance and allows the injectate to be injected within the lesion.

Two post-injection analysis standards were used to provide a comprehensive evaluation of injection accuracy. There were 7 specimens in which disagreement occurred; 5 were scored as successful by gross dissection but as unsuccessful by MRI (MRI false negative) and 2 were scored as successful by MRI but unsuccessful by gross dissection (gross dissection false negative). Therefore, based on a 'success' in at least one modality the overall injection success rate was 90% (80% proximal, 100% distal). However, it was elected to report the results separately to most accurately determine success rate. In this study, assessment of gross sections seemed to be a more sensitive technique to detect the presence of dye within a tendon than MRI. For MRI to detect the presence of fluid, a larger threshold volume seemed to be required. In contrast, only a small amount of colored dye was needed to stain tendon fibers for visualization in gross sections. Thus, evaluation of the gross sections resulted in a higher success rate than MRI evaluation.

Due to the technical difficulty of making thin slices with a band saw, gross dissection sections were made every 1cm, compared to every 5mm for MRI slices. This resulted in imperfect matching of proximal to distal slices between MRI and gross dissection. Thus, in 2 samples, injectate was detected using MRI, but not in gross sections, most likely due to the thicker gross section slice missing the injection site. Mineral oil was selected to inject for its hyperintense signal on T1 imaging and blue and orange dyes were selected as strong and visually distinct colors to represent each location on gross dissection. A standard volume of 3ml was used, which is greater than may be used clinically as the lesion size typically determines volume to be injected. A larger volume was chosen to ensure adequate visibility on post-injection analysis. For all of these reasons, results were reported separately as evaluated by each modality.

In all specimens in this study, at least one synovial structure was marked with injectate on post-injection analysis. The navicular bursa and digital sheath were most commonly involved which is not surprising based on the anatomy of the distal pastern and hoof. [165] The distal dorsal recess of the digital tendon sheath extends down into the hoof capsule to the level of the collateral

sesamoidean ligament. The deep digital flexor tendon tendon is enclosed within a synovial cavity for the majority of its length in the distal limb. In the intrasynovial location, the tendon is only surrounded by epitenon, lacking the more substantial fibrous paratenon layer. Penetration of the needle through the tendon or leakage of injectate through the thin epitenon would result in injection of the sheath at this location. The palmar distal recess of the digital tendon sheath extends to the level of the proximal intertarsal joint, so the needle would likely pass through this pouch before entering the deep digital flexor tendon for a proximal injection. The navicular bursa lies between the palmar surface of the navicular bone and the dorsal surface of the deep digital flexor tendon and extends proximal to the collateral sesamoidean ligament at the medial and lateral aspects. The bursa should not be in the direct path of the needle with this approach, so injection was likely from dorsal penetration of the deep digital flexor tendon with the needle or diffusion of injectate through the dorsal epitenon. As long as aseptic technique is used, penetration of synovial structures is not considered to be a problem.

The treatment options for deep digital flexor tendinopathy are limited, and often dictated by lesion location and type. Conservative therapy results in a poor prognosis for returning to previous levels of athletic performance (25-28%). [1, 4, 9] In contrast, navicular bursoscopy has been recommended as a surgical technique, with improved outcomes of 42% of horses returning to previous level of work. [10] For lesions to be accessible via bursoscopy, they need to be located in the dorsal tendon, within the navicular bursa. For deep digital flexor tendon core lesions, large longitudinal splits or enlarged lobes, intralesional injections have been advocated, with reported use of bone marrow aspirate concentration (BMAC), cultured mesenchymal stem cells (MSCs) or platelet rich plasma (PRP). [17, 89] The majority of research into biologic therapeutics has been performed in the superficial digital flexor tendon, as large core lesions in this tendon are a common injury of performance horses. Experimental, case-controlled studies have been performed *in vivo* with significant improvements seen in histological scores evaluating tissue architecture, fiber pattern and lesion size. [11, 97, 111] A large clinical study investigated the outcomes of racehorses with naturally occurring SDFT lesions, injected with bone marrow-derived MSCs. [14] Cases were compared to historical controls and there was a significant reduction in re-injury rate for MSC treated horses. Other, smaller clinical studies have found similar results with reduced re-injury rate for tendon lesions.[13, 125] In addition, a controlled

clinical study also evaluated morphological and molecular composition of SDF tendons after MSC injection. Significant improvements were seen in structural stiffness and histological scoring of organization, crimp, cellularity, GAG content and vascularity. [12] Overall, evidence for the benefits of intralesional biologic therapeutics is increasing, with the most significant results being improved quality of tendon repair and reduced re-injury rates. The deep digital flexor tendon is intrasynovial through most of the pastern and hoof, thus lacking a paratenon layer. It is hypothesized that tendons heal more slowly when intrasynovial, due to this and the synovial environment. [166] Therefore there may be an increased need for targeted biologic therapeutic preparations for treating lesions in this location.

The reported technique allows for injection of the deep digital flexor tendon within the hoof capsule, a relatively inaccessible location by other imaging modalities. Ultrasonography has been used to evaluate the deep digital flexor tendon down to the level of the proximal and middle phalanx. However, at the level of the middle phalanx, a small convex probe is needed and off-incidence angle results in artifact, as the probe cannot be orientated perpendicular to the tendon fibers. [6, 58] This limitation would make visualizing a needle path very difficult at this level. Furthermore, the small size of the distal pastern requires the needle to be placed without the ultrasound probe in place. With open, low-field MRI, the needle can be placed and following without moving the patient, magnet or radiofrequency coil. A transcuneal approach has also been reported, but visualization is limited to the central third of the distal portion of the deep digital flexor tendon. [58] Currently, there are not any reports of ultrasonographic-guided injection of the distal portion of the DDFT in horses. However, a technique has recently been described to inject the navicular bursa with ultrasonographic-guidance. [167, 168] Some clinicians may be using ultrasonography to guide injection of the DDFT at the level of the collateral sesamoidean ligament and proximal portion of the navicular bursa. A radiographic guided technique has been reported to inject the insertion of the deep digital flexor tendon on midline. [15] This technique can be performed in standing horses, however, it is limited to lesions of the insertion, which occur alone in only 6% of cases. A merit of the reported technique is the potential to inject lesions in standing horses, and to target lesions at any location within the hoof.

In the authors' hospital, the injection technique has been utilized to inject intralesional bone marrow-derived MSCs in 4 clinical cases. No difficulties or complications were noted in these cases, although more clinical cases are needed to ascertain the efficacy of intralesional MSC injection.

The authors conclude that the MRI-guided technique is feasible for injecting the deep digital flexor tendon in standing sedated horses. This was a proof of concept study and the accuracy to inject specific lesions needs to be determined by targeting naturally occurring or experimentally induced tendon lesions. Further clinical trials are also warranted to ascertain which biologic therapeutic preparations are most successful in improving tendon healing.

CONCLUSIONS

The distal portion of the DDFT is a commonly injured soft tissue structure in horses, with a poor prognosis for returning patients to athletic performance without re-injury. The use of biological therapeutics for tendinopathy is increasing, with growing experimental and clinical evidence supporting the efficacy of these products for improving tendon healing. The injection of MSCs directly into a lesion appears to be the most rewarding regenerative therapy option currently available. Although the precise mechanisms by which MSCs contribute to improved healing are not known, histopathology has revealed improvements in tendon organization following MSC injection.

The etiopathogenesis of DDFT injury needs further investigation, as there may be different mechanisms of injury creating different lesions. For example, the DDFT lesions commonly seen with navicular syndrome such as dorsal border lesions, may have a completely different etiology than core lesions. While there has been no overt histological evidence of inflammation in distal DDFT lesions, this is likely due to the inability to examine lesions during the acute phase of injury. Currently there is minimal research using biologic therapeutics in DDFT lesions, but considerable studies investigating the SDFT. It seems likely that the core lesions seen in DDFT lesions may respond similarly to core lesions treated with intralesional injection in the SDFT. Further work to compare specific DDFT lesions with SDFT injury would be interesting to determine if a similar pathogeneis occurs.

Future studies investigating the efficacy of biologic therapeutics need to utilize an improved model of disease which reflects the pre-clinical period of degeneration that occurs, or use naturally occuring tendon injury. The SDFT is used in most experimental studies as this is the most commonly injured soft tissue structure in race horses, and being located in the metacarpal region this tendon is easy to access with ultrasonography. It would be interesting to perform experimental studies using the DDFT to see if lesions of this tendon responded to biologic therapeutics similarly to the SDFT. To further develop the technique for MRI-guided injection of tendon lesions within the hoof capsule, it is important to use the technique in live horses and to have a more precise target such as a core lesion. An experimental, live horse study to induce a focal, core DDFT lesion followed by intralesional injection would be useful. MSCs labeled with

fluroescence dye or superparamagnetic iron oxide nanoparticles could be injected which would allow follow up localization of the stem cells via MRI and histopathology.

Despite an incomplete understanding of the beneficial mechanisms of biologic therapeutics, these preparations are being used routinely in clinical cases of tendinopathy with minimal complications and good clinical results. Therefore it appears reasonable to consider biologic therapeutics for treating DDFT lesions within the hoof. While the accuracy of this injection technique to target a core lesion is not known, the technique is accurate for targeting a specific location within the tendon. In conclusion, this MRI-guided injection technique is highly likely to be clinically useful for treating lesions of the DDFT within the hoof.

REFERENCES

1. Dyson S, Murray R, Schramme MC. Lameness associated with foot pain- results of magnetic resonance imaging in 199 horses (January 2001–December 2003) and response to treatment. *Equine veterinary journal*. 2005;**37**: 113-121.
2. Dyson S, Murray R, Schramme M, Branch M. Lameness in 46 horses associated with deep digital flexor tendonitis in the digit: diagnosis confirmed with magnetic resonance imaging. *Equine veterinary journal*. 2003;**35**: 681-690.
3. Sampson SN, Schneider RK, Gavin PR, Ho CP, Tucker RL, Charles EM. Magnetic resonance imaging findings in horses with recent onset navicular syndrome but without radiographic abnormalities. *Veterinary radiology & ultrasound : the official journal of the American College of Veterinary Radiology and the International Veterinary Radiology Association*. 2009;**50**: 339-346.
4. Cillan-Garcia E, Milner PI, Talbot A, Tucker R, Hendey F, Boswell J, et al. Deep digital flexor tendon injury within the hoof capsule; does lesion type or location predict prognosis? *The Veterinary record*. 2013;**173**: 70.
5. Busoni V, Heimann M, Trenteseaux J, Snaps F, Dondelinger RF. Magnetic resonance imaging findings in the equine deep digital flexor tendon and distal sesamoid bone in advanced navicular disease—an ex vivo study. *Veterinary radiology & ultrasound : the official journal of the American College of Veterinary Radiology and the International Veterinary Radiology Association*. 2005;**46**: 279-286.
6. Mair TS, Kinns JEN. Deep digital flexor tendonitis in the equine foot diagnosed by low-field magnetic resonance imaging in the standing patient: 18 cases. *Veterinary radiology & ultrasound : the official journal of the American College of Veterinary Radiology and the International Veterinary Radiology Association*. 2005;**46**: 458-466.
7. Murray RC, Schramme MC, Dyson SJ, Branch MV, Blunden TS. Magnetic resonance imaging characteristics of the foot in horses with palmar foot pain and control horses. *Veterinary radiology & ultrasound : the official journal of the American College of Veterinary Radiology and the International Veterinary Radiology Association*. 2006;**47**: 1-16.
8. Dyson S, Murray R. Magnetic resonance imaging evaluation of 264 horses with foot pain: The podotrochlear apparatus, deep digital flexor tendon and collateral ligaments of the distal interphalangeal joint. *Equine veterinary journal*. 2007;**39**: 340-343.

9. Vanel M, Olive J, Gold S, Mitchell RD, Walker L. Clinical significance and prognosis of deep digital flexor tendinopathy assessed over time using MRI. *Veterinary radiology & ultrasound : the official journal of the American College of Veterinary Radiology and the International Veterinary Radiology Association*. 2012;**53**: 621-627.
10. Smith MR, Wright IM. Endoscopic evaluation of the navicular bursa: observations, treatment and outcome in 92 cases with identified pathology. *Equine veterinary journal*. 2012;**44**: 339-345.
11. Watts AE, Yeager AE, Kopyov OV, Nixon AJ. Fetal derived embryonic-like stem cells improve healing in a large animal flexor tendonitis model. *Stem cell research & therapy*. 2011;**2**: 4.
12. Smith RK, Werling NJ, Dakin SG, Alam R, Goodship AE, Dudhia J. Beneficial effects of autologous bone marrow-derived mesenchymal stem cells in naturally occurring tendinopathy. *PLoS One*. 2013;**8**: e75697.
13. Guercio A, Di Marco P, Casella S, Russotto L, Puglisi F, Majolino C, *et al*. Mesenchymal Stem Cells Derived From Subcutaneous Fat and Platelet-Rich Plasma Used in Athletic Horses With Lameness of the Superficial Digital Flexor Tendon. *J of Equine Vet Sci*. 2015;**35**: 19-26.
14. Godwin EE, Young NJ, Dudhia J, Beamish IC, Smith RK. Implantation of bone marrow-derived mesenchymal stem cells demonstrates improved outcome in horses with overstrain injury of the superficial digital flexor tendon. *Equine veterinary journal*. 2012;**44**: 25-32.
15. Anderson JDC, Puchalski SM, Larson RF, Delco ML, Snyder JR. Injection of the insertion of the deep digital flexor tendon in horses using radiographic guidance. *Eq Vet Educ*. 2008;**20**: 383-388.
16. Puchalski SM, Snyder JR, Hornof WJ, MacDonald MH, Galuppo LD. Contrast-enhanced computed tomography of the equine distal extremity. *Proceedings of the 51st Annual Convention of the American Association of Equine Practitioners*. Seattle, USA: AAEP, 2005;389-394.
17. Smith MRW, Wright IM, Smith RKW, Bladon B, Schramme MC. Treatment options for DDFT lesions: evidence based results. *Proceedings of the 18th Annual Scientific Meeting of the European College of Veterinary Surgeons*. Nantes, France: ECVS, 2009;211-214.
18. Marcatili M, Marshall J, Voute L. Magnetic resonance imaging-guided injection of platelet-rich plasma for treatment of an insertional core lesion of the deep digital flexor tendon within the foot of a horse. *Eq Vet Educ*. 2016.

19. Hallmarq. Hallmarq Standing Equine MRI. 2016 [cited 2016 June]; Available from: http://www.hallmarq.net/equine

20. Marker DR, P UT, Ungi T, Flammang AJ, Fichtinger G, Iordachita, II, *et al*. MR-guided perineural injection of the ganglion impar: technical considerations and feasibility. *Skeletal Radiol*. 2016;**45**: 591-597.

21. Maurer MH, Disch AC, Hartwig T, Renz DM, Schreiter N, Hamm B, *et al*. Outcome study of real-time MR-guided cervical periradicular injection therapy in an open 1.0 Tesla MRI system. *Cardiovasc Intervent Radiol*. 2014;**37**: 756-762.

22. Voleti PB, Buckley MR, Soslowsky LJ. Tendon healing: repair and regeneration. *Annual review of biomedical engineering*. 2012;**14**: 47-71.

23. Birch HL, Sinclair C, Goodship AE, Smith RKW. Tendon and ligament physiology. In: Hinchcliff KW, Kaneps AJ, Geor RJ (eds): *Equine Sports Medicine and Surgery Basic and clinical sciences of the equine athlete*: Elsevier Ltd., 2014;167-188.

24. Wang JH. Mechanobiology of tendon. *J Biomech*. 2006;**39**: 1563-1582.

25. Auer JA, Stick JA. *Equine Surgery*, 2012.

26. Halasz K, Kassner A, Morgelin M, Heinegard D. COMP acts as a catalyst in collagen fibrillogenesis. *J Biol Chem*. 2007;**282**: 31166-31173.

27. Smith RKW, Gerard M, Dowling B, Dart AJ, Birch HL, Goodship AE. Correlation of cartilage oligomeric matrix protein (COMP) levels in equine tendon with mechanical properties-a proposed role for COMP in determining function-specific mechanical characteristics of locomotor tendons. *Equine veterinary journal*. 2002;**34**: 241-244.

28. Patterson-Kane JC, Parry DAD, Birch HL, Goodship AE, Firth EC. An age-related study of morphology and cross-link composition of collagen fibrils in the digital flexor tendons of young thoroughbred horses. *Connective Tissue Res*. 1997;**36**: 253-260.

29. Smith RKW. Mesenchymal stem cell therapy for equine tendinopathy. *Disability and Rehabilitation*. 2008;**30**: 1752-1758.

30. Cherdchutham W, Becker C, Smith RKW, Barneveld A, van Weeren PR. Age-related changes and effect of exercise on the molecular composition of immature equine superficial digital flexor tendons. *Equine veterinary journal*. 1999;**31**: 86-94.

31. Perkins NR, Reid SW, Morris RS. Risk factors for injury to the superficial digital flexor tendon and suspensory apparatus in Thoroughbred racehorses in New Zealand. *N Z Vet J*. 2005;**53**: 184-192.
32. Patterson-Kane JC, Rich T. Achilles tendon injuries in elite athletes: lessons in pathophysiology from their equine counterparts. *ILAR J*. 2014;**55**: 86-99.
33. Thorpe CT, Streeter I, Pinchbeck GL, Goodship AE, Clegg PD, Birch HL. Aspartic acid racemization and collagen degradation markers reveal an accumulation of damage in tendon collagen that is enhanced with aging. *J Biol Chem*. 2010;**285**: 15674-15681.
34. Dakin SG, Dudhia J, Smith RK. Resolving an inflammatory concept: the importance of inflammation and resolution in tendinopathy. *Vet Immunol Immunopathol*. 2014;**158**: 121-127.
35. Richardson LE, Dudhia J, Clegg PD, Smith R. Stem cells in veterinary medicine--attempts at regenerating equine tendon after injury. *Trends Biotechnol*. 2007;**25**: 409-416.
36. Dakin S. A review of the healing processes in equine superficial digital flexor tendinopathy. *Eq Vet Educ*. 2016.
37. Cook JL, Purdam CR. Is tendon pathology a continuum? A pathology model to explain the clinical presentation of load-induced tendinopathy. *British Journal of Sports Medicine*. 2009;**43**: 409-416.
38. Dakin SG, Dudhia J, Werling NJ, Werling D, Abayasekara DR, Smith RK. Inflamm-aging and arachadonic acid metabolite differences with stage of tendon disease. *PLoS One*. 2012;**7**: e48978.
39. Denoix JM. Functional anatomy of tendons and ligaments in the distal limb (manus and pes). *The Veterinary clinics of North America Equine practice*. 1994;**10**: 273-323.
40. Blunden A, Murray R, Dyson S. Lesions of the deep digital flexor tendon in the digit: A correlative MRI and post mortem study in control and lame horses. *Eq Vet Educ*. 2009;**41**: 25-33.
41. Schramme MC. Deep digital flexor tendonopathy in the foot. *Eq Vet Educ*. 2011;**23**: 403-415.
42. Blunden A, Dyson S, Murray R, Schramme M. Histopathology in horses with chronic palmar foot pain and age-matched controls. Part 2: The deep digital flexor tendon. *Equine veterinary journal*. 2006;**38**: 23-27.
43. Wright IM, Kidd L, Thorp BH. Gross, histological and histomorphometric features of the navicular bone and related structures in the horse *Equine veterinary journal*. 1998;**30**: 220-234.

44. Birch HL, Bailey JVB, Bailey AJ, Goodship AE. Age-related changes to the molecular and cellular components of equine flexor tendons. *Equine veterinary journal*. 1999;**31**: 391-396.
45. Viitanen M, Bird J, Smith R, Tulamo RM, May SA. Biochemical characterisation of navicular hyaline cartilage, navicular fibrocartilage and the deep digital flexor tendon in horses with navicular disease. *Res Vet Sci*. 2003;**75**: 113-120.
46. Beck S, Blunden T, Dyson S, Murray R. Are matrix and vascular changes involved in the pathogenesis of deep digital flexor tendon injury in the horse? *Vet J*. 2011;**189**: 289-295.
47. Beccati F, Pepe M, Pascucci L, Ceccarelli E, Mancini F, Mandara MT. Sympathetic innervation of the suprasesamoidean region of the deep digital flexor tendon in the forelimbs of horses. *Vet J*. 2015;**205**: 413-416
.
48. Dyson S, Murray R, Schramme M, Branch M. Magnetic resonance imaging of the equine foot: 15 horses. *Equine veterinary journal*. 2003;**35**: 18-26.
49. Mair TS, Kinns J, Jones MA, Bolas NM. Magnetic Resonance Imaging of the Distal Limb of the Standing Horse: Technique and Review of 40 Cases of Foot Lameness. *Am Assoc Eq Pract*. New Orleans, 2003;29-41.
50. Mitchell RD, Edwards RB, Makkreel LD, Oliveira TD. Standing MRI Lesions Identified in Jumping and Dressage Horses With Lameness Isolated to the Foot. *Am Assoc Eq Pract*. San Antonio, 2006;422-426.
51. Blunden A, Dyson S, Murray R, Schramme M. Histopathology in horses with chronic palmar foot pain and agematched
controls. Part 1: Navicular bone and related structures. *Equine veterinary journal*. 2006;**38**: 15-22.
52. McCormick JD, Puchalski SM, Schultz RM. Distal Deep Digital Flexor Tendon Angulation and Tendinopathy Within the Equine Foot. *Am Assoc Eq Pract*. San Diego, 2008;232.
53. Eliashar E, McGuigan MP, Wilson AM. Relationship of foot conformation and force applied to the navicular bone of sound horses at the trot. *Equine veterinary journal*. 2004;**36**: 431-435.
54. Smith SS, Dyson S, Murray R. Is There an Association Between Distal Phalanx Angles and Deep Digital Flexor Tendon Lesions? : *Am Assoc Eq Pract*, 2004;328-331.

55. Dyson S, Murray R, Schramme M, Branch M. Collateral desmitis of the distal interphalangeal joint in 18 horses (2001–2002). *Equine veterinary journal*. 2004;**36**: 160-166.
56. Milner PI, Sidwell S, Talbot AM, Clegg PD. Short-term temporal alterations in magnetic resonance signal occur in primary lesions identified in the deep digital flexor tendon of the equine digit. *Equine veterinary journal*. 2012;**44**: 157-162.
57. Seignour M, Pasquet H, Coudry V, Denoix JM. Ultrasonographic diagnosis of injuries to the deep digital flexor tendon and associated structures in the equine foot (suprasesamoidean area). *Eq Vet Educ*. 2011;**23**: 369-376.
58. Whitcomb MB. Ultrasonographic Evaluation of the Distal Extremity. *J Eq Vet Sci*. 2009;**29**: 47-59.
59. Dyson S, Murray R. Use of concurrent scintigraphic and magnetic resonance imaging evaluation to improve understanding of the pathogenesis of injury of the podotrochlear apparatus. *Equine veterinary journal*. 2007;**39**: 365-369.
60. Martinelli MJ, Rantanen NW. Relationship Between Nuclear Scintigraphy and Standing MRI in 30 Horses With Lameness of the Foot. *Am Assoc Eq Pract*. Seattle, 2005;359.
61. Bolas N. Basic MRI principals. In: Murray R (ed): *Equine MRI*. West Sussex: Blackwell Publishing Ltd, 2011.
62. Schild HH. *MRI made easy*. Berlin: Schering AG, 1990.
63. Werpy N. Low-field MRI in horses: practicalities and image acquisition. In: Murray R (ed): *Equine MRI*. West Sussex: Blackwell Publishing Ltd., 2011.
64. Spriet M, McKnight A. Characterization of the magic angle effect in the equine deep digital flexor tendon using a low-field magnetic resonance system. *Veterinary radiology & ultrasound : the official journal of the American College of Veterinary Radiology and the International Veterinary Radiology Association*. 2009;**50**: 32-36.
65. Murray RC, Roberts BL, Schramme MC, Dyson SJ, Branch M. Quantitative Evaluation of Equine Deep Digital Flexor Tendon Morphology using Magnetic Resonance Imaging. *Veterinary radiology & ultrasound : the official journal of the American College of Veterinary Radiology and the International Veterinary Radiology Association*. 2004;**45**: 103-111.
66. Maher MC, Werpy NM, Goodrich LR, McIllwraith CW. Distention of the navicular bursa to determine the presence of adhesions using magnetic resonance imaging. *AAEP Convention*. San Diego, 2008;460-461.

67. Judy CE, Saveraid TC, Rick MC. Characterization of Foot Lesions Using Contrast Enhanced Equine Orthopedic Magnetic Resonance Imaging. *Am Assoc Eq Pract*. San Diego, 2008;459.
68. Tietje S, Nowak M, Petzoldt S, Weiler H. Die computertomographische Darstellung des distalen Abschnitts der tiefen Beugesehne (TBS) des Pferdes. *Pferdeheilkunde*. 2001;**17**: 21-29.
69. van Hamel SE, Bergman HJ, Puchalski SM, de Groot MW, van Weeren PR. Contrast-enhanced computed tomographic evaluation of the deep digital flexor tendon in the equine foot compared to macroscopic and histological findings in 23 limbs. *Equine veterinary journal*. 2014;**46**: 300-305.
70. Vallance SA, Bell RJ, Spriet M, Kass PH, Puchalski SM. Comparisons of computed tomography, contrast-enhanced computed tomography and standing low-field magnetic resonance imaging in horses with lameness localised to the foot. Part 2: Lesion identification. *Equine veterinary journal*. 2012;**44**: 149-156.
71. Puchalski SM, Galuppo LD, Drew CP, Wisner ER. Use of Contrast-Enhanced Computed Tomography to Assess Angiogenesis in Deep Digital Flexor Tendonopathy in a Horse. *Veterinary radiology & ultrasound : the official journal of the American College of Veterinary Radiology and the International Veterinary Radiology Association*. 2009;**50**: 292-297.
72. Smith LCR. Use of interventional imaging in equine veterinary medicine. *Eq Vet Educ*. 2013;**25**: 177-178.
73. Lustgarten M, Redding WR, Schnabel LV, Prange T, Seiler GS. Navigational ultrasound imaging: A novel imaging tool for aiding interventional therapies of equine musculoskeletal injuries. *Equine veterinary journal*. 2016;**48**: 195-200.
74. Mettenleiter E. Interventionelle Computertomographie – eine neue Dimension in der Pferdemedizin – Teil 1: CT-gesteuerte Aufbohrung und Füllung subchondraler Knochenzysten beim Pferd. *Pferdeheilkunde*. 2014;**30**: 567-576.
75. DeAngelis GA, Moran RE, Fajardo LL, Mugler JP, Christopher JM, Harvey JA. MRI-Guided Needle Localization: Technique. *Seminars in Ultrasound, CT, and MRI*. 2000;**21**: 337-350.
76. Moche M, Zajonz D, Kahn T, Busse H. MRI-guided procedures in various regions of the body using a robotic assistance system in a closed-bore scanner: preliminary clinical experience and limitations. *J Magn Reson Imaging*. 2010;**31**: 964-974.

77. Lamb ML, Barrett JG, White NA, II, Werre SR. Accuracy Of Low-Field Magnetic Resonance Imaging Versus Radiography For Guiding Injection Of Equine Distal Interphalangeal Joint Collateral Ligaments. *Veterinary radiology & ultrasound : the official journal of the American College of Veterinary Radiology and the International Veterinary Radiology Association*. 2014;**55**: 174-181.
78. White NAI, Barrett JG. Magnetic Resonance Imaging-Guided Treatment of Equine Distal Interphalangeal Joint Collateral Ligaments: 2009–2014. *Front Vet Sci*. 2016;**3**.
79. Sequeiros RB, Ojala RO, Klemola R, Vaara TJ, Jyrkinen L, Tervonen OA. MRI-guided periradicular nerve root infiltration therapy in low-field (0.23-T) MRI system using optical instrument tracking. *Eur Radiol*. 2002;**12**: 1331-1337.
80. Schramme MC. Treatment of deep digital flexor tendonitis in the foot. *Eq Vet Educ*. 2008;**20**: 389-391.
81. Johnston GM, Taylor PM, Holmes MA, Wood JLN. Confidential enquiry of peri-operative equine fatalities (CEPEF): preliminary results. *Equine veterinary journal*. 1995;**27**: 193-200.
82. Murray RC, Mair TS, Sherlock CE, Blunden AS. Comparison of high-field and low-field magnetic resonance images of cadaver limbs of horses. *The Veterinary record*. 2009;**165**: 281-200.
83. Lutter JD, Schneider RK, Sampson SN, Cary JA, Roberts GD, Vahl CI. Medical treatment of horses with deep digital flexor tendon injuries diagnosed with high-field-strength magnetic resonance imaging- 118 cases. *J Am Vet Assoc*. 2015;**247**: 1309-1318.
84. Schneider RK, Gavin PR, Tucker RL. What MRI is teaching us about navicular disease. *Am Assoc Eq Pract*. New Orleans, 2003;210-219.
85. Marsh CA, Schneider RK, Sampson SN, Roberts GD. Response to injection of the navicular bursa with corticosteroid and hyaluronan following high-field magnetic resonance imaging in horses with signs of navicular syndrome- 101 cases (2000–2008). *J Am Vet Assoc*. 2012;**241**: 1353-1364.
86. Bell CD, Howard RD, Taylor S, Voss ED, Werpy N. Outcomes of podotrochlear (navicular) bursa injections for signs of foot pain in horses evaluated via magnetic resonance imaging: 23 cases (2005–2007). *J Am Vet Assoc*. 2009;**234**: 920-925.

87. Howlinski M, Judy C, Saveraid T, Maranda L. Resolution of lesions on STIR images is associated with improved lameness status in horses. . *Veterinary radiology & ultrasound : the official journal of the American College of Veterinary Radiology and the International Veterinary Radiology Association*. 2010;**51**: 479-484.
88. Schneider RK, Gavin PR, Tucker RL. What MRI is teaching us about navicular disease. Lexington: American Association of Equine Practitioners (AAEP), 2003;210-219.
89. Maher O, Snyder JR, Symms WA, Puchalski SM. Deep digital flexor tendon injuries in the equine foot. *Proceedings of the American College of Veterinary Surgeons Veterinary Symposium*. Chicago, USA: ACVS, 2007;92-93.
90. Humbach KE, Gutierrez-Nibeyro SD. Desmotomy of the accessory ligament of the deep digital flexor tendon for treatment of chronic deep digital flexor tendinopathy in three Quarter Horses. *Eq Vet Educ*. 2017.
91. Nixon AJ. Treatment options after MRI imaging. *Am Coll Vet Surg*. Washington DC, 2009;53-60.
92. Dabareiner RM, Carter K, Honnas CM. Injection of corticosteroids, hyaluronate, and amikacin into the navicular bursa in horses with signs of navicular area pain unresponsive to other treatments: 25 cases (1999–2002). *J Am Vet Assoc*. 2003;**223**: 1469-1474.
93. Shrier I, Matheson GO, Khol HW. Achilles tendonitis: Are corticosteroid injections useful or harmful? *Clinical Journal of Sports Medicine*. 1996: 245-250.
94. Swanstrom MD, Stover SM, Hubbard M, Hawkins DA. Determination of passive mechanical properties of the superficial and deep digital flexor muscle-ligament-tendon complexes in the forelimbs of horses. *Am J Vet Res*. 2004;**65**: 188-197.
95. Fortier LA, Smith RKW. Regenerative medicine for tendinous and ligamentous injuries of sport horses. *The Veterinary clinics of North America Equine practice*. 2008;**24**: 191-201.
96. Volk SW, Theoret C. Translating stem cell therapies: the role of companion animals in regenerative medicine. *Wound repair and regeneration : official publication of the Wound Healing Society [and] the European Tissue Repair Society*. 2013;**21**: 382-394.
97. Nixon AJ, Dahlgreen LA, Haupt JL, Yeager AE, Ward DL. Effect of adipose-derived nucleated cell fractions on tendon repair in horses with collagenase-induced tendinitis. *Am J Vet Res*. 2008;**69**: 928-937.

98. Crovace A, Lacitignola L, Rossi G, Francioso E. Histological and immunohistochemical evaluation of autologous cultured bone marrow mesenchymal stem cells and bone marrow mononucleated cells in collagenase-induced tendinitis of equine superficial digital flexor tendon. *Veterinary medicine international*. 2010;**2010**: 250978.
99. Smith RK. 'Can you regain your youth?'--the real potential of stem cell technology. *Equine veterinary journal*. 2010;**42**: 2-4.
100. De Schauwer C. Towards a uniform characterization of equine mesenchymal stromal cells. Dissertation. Ghent University, Belgium, 2012.
101. Breton A, Sharma R, Diaz AC, Parham AG, Graham A, Neil C, *et al.* Derivation and characterization of induced pluripotent stem cells from equine fibroblasts. *Stem Cells Dev*. 2013;**22**: 611-621.
102. Watts AE. Use of stem cells in equine musculoskeletal disorders. *Eq Vet Educ*. 2014;**26**: 492-498.
103. Lopez MJ, Jarazo J. State of the art: Stem cells in equine regenerative medicine. *Equine veterinary journal*. 2014.
104. Caplan AI, Dennis JE. Mesenchymal stem cells as trophic mediators. *J Cell Biochem*. 2006;**98**: 1076-1084.
105. Dominici M, Le Blanc K, Mueller I, Slaper-Cortenbach I, Marini F, Krause D, *et al*. Minimal criteria for defining multipotent mesenchymal stromal cells. The International Society for Cellular Therapy position statement. *Cytotherapy*. 2006;**8**: 315-317.
106. Guest DJ, Smith MRW, Allen WR. Equine embryonic stem-like cells and mesenchymal stromal cells have different survival rates and migration patterns following their injection into damaged superficial digital flexor tendon. *Equine veterinary journal*. 2010;**42**: 636-642.
107. Scharf A, Holmes SP, Thoresen M, Mumaw J, Stumpf A, Peroni J. MRI-Based Assessment of Intralesional Delivery of Bone Marrow-Derived Mesenchymal Stem Cells in a Model of Equine Tendonitis. *Stem Cells International*. 2016;**2016**.
108. Berner D, Brehm W, Gerlach K, Gittel C, Offhaus J, Paebst F, *et al*. Longitudinal Cell Tracking and Simultaneous Monitoring of Tissue Regeneration after Cell Treatment of Natural Tendon Disease by Low-Field Magnetic Resonance Imaging. *Stem Cells Int*. 2016;**2016**: 1207190.

109. Becerra P, Valdes Vazquez MA, Dudhia J, Fiske-Jackson AR, Neves F, Hartman NG, *et al*. Distribution of injected technetium(99m)-labeled mesenchymal stem cells in horses with naturally occurring tendinopathy. *Journal of orthopaedic research : official publication of the Orthopaedic Research Society*. 2013;**31**: 1096-1102.
110. Caplan AI. Adult mesenchymal stem cells for tissue engineering versus regenerative medicine. *J Cell Physiol*. 2007;**213**: 341-347.
111. Schnabel LV, Lynch ME, van der Meulen MC, Yeager AE, Kornatowski MA, Nixon AJ. Mesenchymal stem cells and insulin-like growth factor-I gene-enhanced mesenchymal stem cells improve structural aspects of healing in equine flexor digitorum superficialis tendons. *Journal of orthopaedic research : official publication of the Orthopaedic Research Society*. 2009;**27**: 1392-1398.
112. Pittenger MF, Mackay AM, Beck SC, Jaiswal RK, Douglas R, Mosca JD, *et al*. Multilineage Potential of Adult Human Mesenchymal Stem Cells. *Science*. 1999;**284**: 143-147.
113. Stolzing A, Jones E, McGonagle D, Scutt A. Age-related changes in human bone marrow-derived mesenchymal stem cells: consequences for cell therapies. *Mech Ageing Dev*. 2008;**129**: 163-173.
114. Vidal MA, Kilroy GE, Johnson JR, Lopez MJ, Moore RM, Gimble JM. Cell growth characteristics and differentiation frequency of adherent equine bone marrow-derived mesenchymal stromal cells: adipogenic and osteogenic capacity. *Vet Surg*. 2006;**35**: 601-610.
115. Delling U, Lindner K, Ribitsch I, Julke H, Brehm W. Comparison of bone marrow aspiration at the sternum and the tuber coxae in middle-aged horses. *Canadian J Vet Res*. 2012;**76**: 52-56.
116. Kisiday JD, Goodrich LR, Mcllwraith W, Frisbie DD. Effects of equine bone marrow aspirate volume on isolation, proliferation, and differentiation potential of mesenchymal stem cells. *Am J Vet Res*. 2013;**74**: 801-807.
117. Durando MM, Zarucco L, Schaer TP, Ross MW, Reef VB. Pneumopericardium in a horse secondary to sternal bone marrow aspiration. *Eq Vet Educ*. 2006;**18**: 75-79.
118. Kasashima Y, Ueno T, Tomita A, Goodship AE, Smith RKW. Optimisation of bone marrow aspiration from the equine sternum for the safe recovery of mesenchymal stem cells. *Equine veterinary journal*. 2010;**43**: 288-294.

119. Peters AE, Watts AE. Biopsy Needle Advancement during Bone Marrow Aspiration Increases Mesenchymal Stem Cell Concentration. *Front Vet Sci*. 2016;**3**: 23.
120. Ishihara A, Helbig HJ, Sanchez-Hodge RB, Wellman ML, D. LM, Bertone AL. Performance of a gravitational marrow separator, multidirectional bone marrow aspiration needle, and repeated bone marrow collections on the production of concentrated bone marrow and separation of mesenchymal stem cells in horses. *Am J Vet Res*. 2013;**74**: 854-863.
121. Hildebrand KA, Jia F, Woo SL. Response of donor and recipient cells after transplantation of cells to the ligament and tendon. *Microsc Res Tech*. 2002;**58**: 34-38.
122. Butler DL, Juncosa-Melvin N, Boivin GP, Galloway MT, Shearn JT, Gooch C, *et al.* Functional tissue engineering for tendon repair: A multidisciplinary strategy using mesenchymal stem cells, bioscaffolds, and mechanical stimulation. *Journal of orthopaedic research : official publication of the Orthopaedic Research Society*. 2008;**26**: 1-9.
123. Butler DL, Gooch C, Kinneberg KR, Boivin GP, Galloway MT, Nirmalanandhan VS, *et al*. The use of mesenchymal stem cells in collagen-based scaffolds for tissue-engineered repair of tendons. *Nat Protoc*. 2010;**5**: 849-863.
124. Awad HA, Boivin GP, Dressler MR, Smith FNL, Young RG, Butler DL. Repair of patellar tendon injuries using a cell-collagen composite. *Journal of orthopaedic research : official publication of the Orthopaedic Research Society*. 2003;**21**: 420-431.
125. Pacini S, Spinabella S, Trombi L, Fazzi R, Galimberti S, Dini F, *et al*. Suspension of bone marrow-derived undifferentiated mesenchymal stromal cells for repair of superficial digital flexor tendon in race horses. *Tissue Eng*. 2007;**13**: 2949-2955.
126. Caniglia CJ, Schramme MC, Smith RK. The effect of intralesional injection of bone marrow derived mesenchymal stem cells and bone marrow supernatant on collagen fibril size in a surgical model of equine superficial digital flexor tendonitis. *Equine veterinary journal*. 2012;**44**: 587-593.
127. Vidal MA, Kilroy GE, Lopez MJ, Johnson JR, Moore RM, Gimble JM. Characterization of equine adipose tissue-derived stromal cells: adipogenic and osteogenic capacity and comparison with bone marrow-derived mesenchymal stromal cells. *Vet Surg*. 2007;**36**: 613-622.
128. Raabe O, Shell K, Wurtz A, Reich CM, Wenisch S, Arnhold S. Further insights into the characterization of equine adipose tissue-derived mesenchymal stem cells. *Vet Res Commun*. 2011;**35**: 355-365.

129. Stewart MC, Stewart AA. Mesenchymal stem cells: characteristics, sources, and mechanisms of action. *The Veterinary clinics of North America Equine practice*. 2011;**27**: 243-261.
130. Burk J, Gittel C, Heller S, Pfeiffer B, Paebst F, Ahrberg A, *et al.* Gene expression of tendon markers in mesenchymal stromal cells derived from different sources. *BMC Research Notes*. 2014;**7**: 826-832.
131. Borjesson DL. The Regenerative Medicine Laboratory- Facilitating Stem Cell Therapy for Equine Disease. *Clin Lab Med*. 2011;**31**: 109-123.
132. Youngstrom DW, LaDow JE, Barrett JG. Tenogenesis of bone marrow-, adipose-, and tendon-derived stem cells in a dynamic bioreactor. *Connective Tissue Res*. 2016;**57**: 454 - 465.
133. Alipour F, Parham A, Mehrjerdi HK, Dehghani H. Equine Adipose-Derived Mesenchymal Stem Cells- Phenotype and Growth Characteristics, Gene Expression Profile and Differentiation Potentials. *Cell Journal*. 2015;**16**: 456-465.
134. Gittel C, Brehm W, Burk J, Juelke H, Staszyk C, Ribitsch I. Isolation of equine multipotent mesenchymal stromal cells by enzymatic tissue digestion or explant technique: comparison of cellular properties. *BMC Vet Res*. 2013;**9**: 221-235.
135. Geburek F, Mundle K, Conrad S, Hellige M, Walliser U, van Schie HT, *et al*. Tracking of autologous adipose tissue-derived mesenchymal stromal cells with *in vivo* magnetic resonance imaging and histology after intralesional treatment of artificial equine tendon lesions--a pilot study. *Stem cell research & therapy*. 2016;**7**: 21.
136. Carvalho AM, Yamada AL, Golim MA, Alvarez LE, Hussni CA, Alves AL. Evaluation of mesenchymal stem cell migration after equine tendonitis therapy. *Equine veterinary journal*. 2014;**46**: 635-638.
137. Conze P, van Schie HT, van Weeren R, Staszyk C, Conrad S, Skutella T, *et al*. Effect of autologous adipose tissue-derived mesenchymal stem cells on neovascularization of artificial equine tendon lesions. *Regen Med*. 2014;**9**: 743-757.
138. Carvalho AM, Alves ALG, de Oliveria PGG, Alvarez LEC, Amorim RL, Hussni CA, *et al*. Use of Adipose Tissue-Derived Mesenchymal Stem Cells for Experimental Tendinitis Therapy in Equines. *J Eq Vet Sci*. 2011;**31**: 26-34.
139. Ricco S, Renzi S, Del Bue M, Conti V, Merli E, Ramoni R, *et al*. Allogeneic adipose tissue-derived mesenchymal stem cells in combination with platelet rich plasma are safe and

effective in the therapy of superficial digital flexor tendonitis in the horse. . *Int J Immunopathol Pharmacol*. 2013;**26**: 61-68.

140. Del Bue M, Ricco S, Ramoni R, Conti V, Gnudi G, Grolli S. Equine adipose-tissue derived mesenchymal stem cells and platelet concentrates: their association *in vitro* and *in vivo*. *Vet Res Commun*. 2008;**32 Suppl 1**: S51-55.

141. Guest DJ, Smith MR, Allen WR. Equine embryonic stem-like cells and mesenchymal stromal cells have different survival rates and migration patterns following their injection into damaged superficial digital flexor tendon. *Equine veterinary journal*. 2010;**42**: 636-642.

142. Paterson YZ, Rash N, Garvican ER, Palliot R, Guest DJ. Equine mesenchymal stromal cells and embryo-derived stem cells are immune privileged *in vitro*. *Stem cell research & therapy*. 2014;**5**: 90-103.

143. Lepage SI, Nagy K, Sung HK, Kandel RA, Nagy A, Koch TG. Generation, Characterization, and Multilineage Potency of Mesenchymal-Like Progenitors Derived from Equine Induced Pluripotent Stem Cells. *Stem Cells Dev*. 2016;**25**: 80-89.

144. Aguiar C, Theoret C, Smith O, Segura M, Lemire P, Smith LC. Immune potential of allogeneic equine induced pluripotent stem cells. *Equine veterinary journal*. 2015;**47**: 708-714.

145. Andia I, Sanchez M, Maffulli N. Tendon healing and platelet-rich plasma therapies. *Expert Opin, Biol Ther*. 2010;**10**: 1415-1426.

146. DeLong JM, Russell RP, Mazzocca AD. Platelet-rich plasma: the PAW classification system. *Arthroscopy*. 2012;**28**: 998-1009.

147. McCarrel TM, Minas T, Fortier LA. Optimization of leukocyte concentration in platelet-rich plasma for the treatment of tendinopathy. *J Bone Joint Surg Am*. 2012;**94**: e143(141-148).

148. Sundman EA, Cole BJ, Fortier LA. Growth factor and catabolic cytokine concentrations are influenced by the cellular composition of platelet-rich plasma. *Am J Sports Med*. 2011;**39**: 2135-2140.

149. Boswell SG, Schnabel LV, Mohammed HO, Sundman EA, Minas T, Fortier LA. Increasing platelet concentrations in leukocyte-reduced platelet-rich plasma decrease collagen gene synthesis in tendons. *Am J Sports Med*. 2014;**42**: 42-49.

150. Bosch G, Moleman M, Barneveld A, van Weeren PR, van Schie HT. The effect of platelet-rich plasma on the neovascularization of surgically created equine superficial digital flexor tendon lesions. *Scand J Med Sci Sports*. 2011;**21**: 554-561.

151. Schnabel LV, Mohammed HO, Miller BJ, McDermott WG, Jacobson MS, Santangelo KS, *et al*. Platelet rich plasma (PRP) enhances anabolic gene expression patterns in flexor digitorum superficialis tendons. *Journal of orthopaedic research : official publication of the Orthopaedic Research Society*. 2007;**25**: 230-240.
152. Anitua E, Andia I, Sanchez M, Azofra J, del Mar Zalduendo M, de la Fuente M, *et al*. Autologous preparations rich in growth factors promote proliferation and induce VEGF and HGF production by human tendon cells in culture. *Journal of orthopaedic research : official publication of the Orthopaedic Research Society*. 2005;**23**: 281-286.
153. Lyras DN, Kazakos K, Verettas D, Botaitis S, Agrogiannis G, Kokka A, *et al*. The effect of platelet-rich plasma gel in the early phase of patellar tendon healing. *Arch Orthop Trauma Surg*. 2009;**129**: 1577-1582.
154. Aspenburg P, Virchenko O. Platelet concentrate injection improves Achilles tendon repair in rats. *Acta Orthop Scand*. 2004;**75**: 93-99.
155. de Voss RJ, Weir A, van Schie HTM, Bierma-Zeinstra SMA, Verhaar JAN, Tol JL. Platelet-Rich Plasma Injection for Chronic Achilles Tendinopathy. *J Am Med Assoc*. 2010;**303**: 144-149.
156. Mishra A, Pavelko T. Treatment of chronic elbow tendinosis with buffered platelet-rich plasma. *Am J Sports Med*. 2006;**34**: 1774-1778.
157. Peerbooms JC, Sluimer J, Bruijn DJ, Gosens T. Positive effect of an autologous platelet concentrate in lateral epicondylitis in a double-blind randomized controlled trial: platelet-rich plasma versus corticosteroid injection with a 1-year follow-up. *Am J Sports Med*. 2010;**38**: 255-262.
158. Bosch G, van Schie HT, de Groot MW, Cadby JA, van de Lest CH, Barneveld A, *et al*. Effects of platelet-rich plasma on the quality of repair of mechanically induced core lesions in equine superficial digital flexor tendons: A placebo-controlled experimental study. *Journal of orthopaedic research : official publication of the Orthopaedic Research Society*. 2010;**28**: 211-217.
159. Maia L, de Souza MV, Junior JIR, de Oliveria AC, Alves GES, Benjamin LA, *et al*. Platelet-Rich Plasma in the Treatment of Induced Tendinopathy in Horses- Histologic Evaluation. *J Eq Vet Sci*. 2009;**29**: 618-626.

160. Cadby JA, David F, van de Lest C, Bosch G, van Weeren PR, Snedeker JG, *et al*. Further characterisation of an experimental model of tendinopathy in the horse. *Equine veterinary journal*. 2013;**45**: 642-648.
161. Martinello T, Bronzini I, Perazzi A, Testoni S, De Benedictis GM, Negro A, *et al*. Effects of *in vivo* applications of peripheral blood-derived mesenchymal stromal cells (PB-MSCs) and platlet-rich plasma (PRP) on experimentally injured deep digital flexor tendons of sheep. *Journal of orthopaedic research : official publication of the Orthopaedic Research Society*. 2013;**31**: 306-314.
162. Carvalho AM, Badial PR, Alvarez LEC, Yamada ALM, Borges AS, Deffune E, *et al*. Equine tendonitis therapy using mesenchymal stem cells and platelet concentrates- a randomized controlled trial. *Stem cell research & therapy*. 2013;**4**: 85-98.
163. Estrada RJ, van Weeren R, van de Lest CH, Boere J, Reyes M, Ionita JC, *et al*. Effects of Autologous Conditioned Plasma® (ACP) on the healing of surgically induced core lesions in equine superficial digital flexor tendon. *Pferdeheilkunde*. 2014;**30**: 633-642.
164. Bosch G, Rene van Weeren P, Barneveld A, van Schie HT. Computerised analysis of standardised ultrasonographic images to monitor the repair of surgically created core lesions in equine superficial digital flexor tendons following treatment with intratendinous platelet rich plasma or placebo. *Vet J*. 2011;**187**: 92-98.
165. Denoix JM. *The Equine Distal Limb: An atlas of clinical anatomy and comparitive imaging*. Iowa: Iowa State University Press, 2000.
166. Avella CS, Smith RKW. Diagnosis and management of tendon and ligament disorders. In: Auer JA, Stick JA (eds): *Equine Surgery*. Missouri: Elsevier Saunders, 2012.
167. Perrin R, Diguet AC, Cantet P, Bailly C, Brogniez L, Dugdale A, *et al*. Ex Vivo Assessment of an Ultrasound-Guided Injection Technique of the Navicular Bursa in the Horse. *Anat Histol Embryol*. 2016;**45**: 450-456.
168. Estrada RJ, Pascual A, Lischer CJ. Development and Evaluation of Ultrasound-Guided Navicular Bursa Injection Using the Palmarodistal Digital Approach in Horses- an Ex Vivo Study. *J Eq Vet Sci*. 2015;**35**: 849-855.